

AD/A-005 222

A FLUX CIRCUIT ANALYSIS FOR THE  
MAGNETIC TRANSDUCER OF A FLUIDIC  
REED GENERATOR

Herbert A. Leupold, et al

Harry Diamond Laboratories

Prepared for:

Army Electronics Command

January 1975

DISTRIBUTED BY:



National Technical Information Service  
U. S. DEPARTMENT OF COMMERCE

Best Available Copy



## NOTICES

### Disclaimers

The findings in this report are not to be construed as an official Department of the Army position, unless so designated by other authorized documents.

The citation of trade names and names of manufacturers in this report is not to be construed as official Government endorsement or approval of commercial products or services referenced herein.

### Disposition

Destroy this report when it is no longer needed. Do not return it to the originator.

16

Best Available Copy

Unclassified

SECURITY CLASSIFICATION OF THIS PAGE (When Data Entered)

REPORT DOCUMENTATION PAGE		READ INSTRUCTIONS BEFORE COMPLETING FORM
1. REPORT NUMBER ECCM-1,2NL	2. GOVT ACCESSION NO.	3. RECIPIENT'S CATALOG NUMBER ADIA 005222
4. TITLE (and Subtitle) A FLUX CIRCUIT ANALYSIS FOR THE MAGNETIC TRANSDUCER OF A FLUIDIC REED GENERATOR		5. TYPE OF REPORT & PERIOD COVERED
7. AUTHOR(S) Herbert A. Leupold Frederick Rothwarf Doyle Edriston		6. PERFORMING ORG. REPORT NUMBER
8. CONTRACT OR GRANT NUMBER(S)		9. PERFORMING ORGANIZATION NAME AND ADDRESS Electronic Materials & Nuclear Hardening Rsch Area US Army Electronics Technology & Devices Lab (ECCM) Fort Monmouth, NJ 07703 AMSEL-TL-ES
10. PROGRAM ELEMENT, PROJECT, TASK AREA & WORK UNIT NUMBERS Proj. No. 1W663613DE5506 Pron No. A9-4-00068-01A9-CT		11. CONTROLLING OFFICE NAME AND ADDRESS Harry Diamond Laboratories Connecticut Ave. at Van Ness NW Washington, DC 20438
12. REPORT DATE 1 JUN 73		13. NUMBER OF PAGES 55
14. MONITORING AGENCY NAME & ADDRESS (if different from Controlling Office)		15. SECURITY CLASS (of this report) Unclassified
16. DISTRIBUTION STATEMENT (of this Report)  Approved for public release; distribution unlimited.		17. DECLASSIFICATION DOWNGRADING SCHEDULE
18. SUPPLEMENTARY NOTES  <b>PRICES SUBJECT TO CHANGE</b>		
19. KEY WORDS (Continue on reverse side if necessary and identify by block number) Artillery Fuze Fluidic Generator Magnetic Permeances Eddy Current Losses		
20. ABSTRACT (Continue on reverse side if necessary and identify by block number) A mathematical analysis is made of the magnetic circuit of a fluidic generator to be used in various fusing applications. A method for obtaining the approximate power output of a prototype generator as a function of the relevant geometric parameters is developed, and sample calculations are made for some typical values of these parameters. In the present design the calculations show that both the vibrating reed and part of the magnet keeper are magnetically saturated under projected operating conditions with the result that only about 35% of the potential power output is actually realized. (Cont'd on reverse side)		

DD FORM 1 JAN 73 1473

NATIONAL TECHNICAL  
INFORMATION SERVICE

U.S. Government of Commerce  
GSA GEN. REG. NO. 22151

Unclassified

SECURITY CLASSIFICATION OF THIS PAGE (When Data Entered)

**UNCLASSIFIED**

SECURITY CLASSIFICATION OF THIS PAGE (When Data Entered)

**20. Abstract (cont'd)**

Experimental data verify this conclusion, as agreement with the calculated value of power is better than 1%. Losses due to eddy currents and hysteresis are found to be much less serious amounting to no more than a few percent. Recommendations of possible remedies for the saturation problem are made. A computer study is made to determine the effect of variation of the relevant design parameters on the peak voltage output of the generator. The resulting design matrices provide a useful guide to design optimization as well as a clear delineation between the parameter combinations which result in saturation of the reed material and those which do not. Recommendations are made for design changes to improve the generator performance.

10

**UNCLASSIFIED**

SECURITY CLASSIFICATION OF THIS PAGE (When Data Entered)

## CONTENTS

	<u>Page</u>
INTRODUCTION	1
THE MAGNETIC CIRCUIT EQUATIONS	2
THE PERMEANCE CALCULATIONS	4
CALCULATIONS OF GAP FLUX DENSITIES IN THE ABSENCE OF A REED	17
SAMPLE CALCULATION FOR POWER OUTPUT IN THE LOAD RESISTANCE $R_L$	19
EXPERIMENTAL CHECK OF CALCULATIONS	26
LOSSES IN THE REED	27
LOSSES IN THE KEEPER	28
SUMMARY AND RECOMMENDATIONS	29
APPENDIX I	32
APPENDIX II	35

## TABLES

I. Fixed Dimensions of Generator Configuration and Values of Critical Constants	7
II. Voltage Outputs for Various Gap Lengths, Reed Thicknesses and Reed Displacement Amplitudes	41-49

## FIGURES

1. Schematic View of Fluidic Generator with Reed Type Magnetic Transducer	1
2. Schematic Representation of the Magnetic Circuit and its Analogue	2
3. Fluidic Generator	5
4. Sectional View of Fluidic Generator in Projectile Ogive	6
5. Calculation of the Relevant Permeances	8
6. Calculation of the Permeance $P_{M4}$	9
7. Determination of the Width $y_p$ in the Formula for Permeance $P_{L3}$	14

	<u>Page</u>
8. Determination of the Inner Flux Paths Comprising Permeance $P_{M4}$	18
9. Determination of B for a Fluidic Generator with a .070" Gap Length	20
10. Comparison of Experimental Points with Theoretical EMF-Displacement Curve	27
11. Inductance of Sensing Coil as a Function of Reed Thickness	31
12. Derivation of the Eddy Current Loss Formula	33

## A FLUX CIRCUIT ANALYSIS FOR THE MAGNETIC TRANSDUCER OF A FLUIDIC REED GENERATOR

### INTRODUCTION

There is considerable interest in the utilization of fluidic generators in various fusing applications.<sup>1-3</sup> These devices are mounted in the ogives of various projectiles and they essentially convert some of the energy of the relative motion of projectile and air first into acoustical energy and thence to electrical energy. A typical device is pictured schematically in Fig. 1.

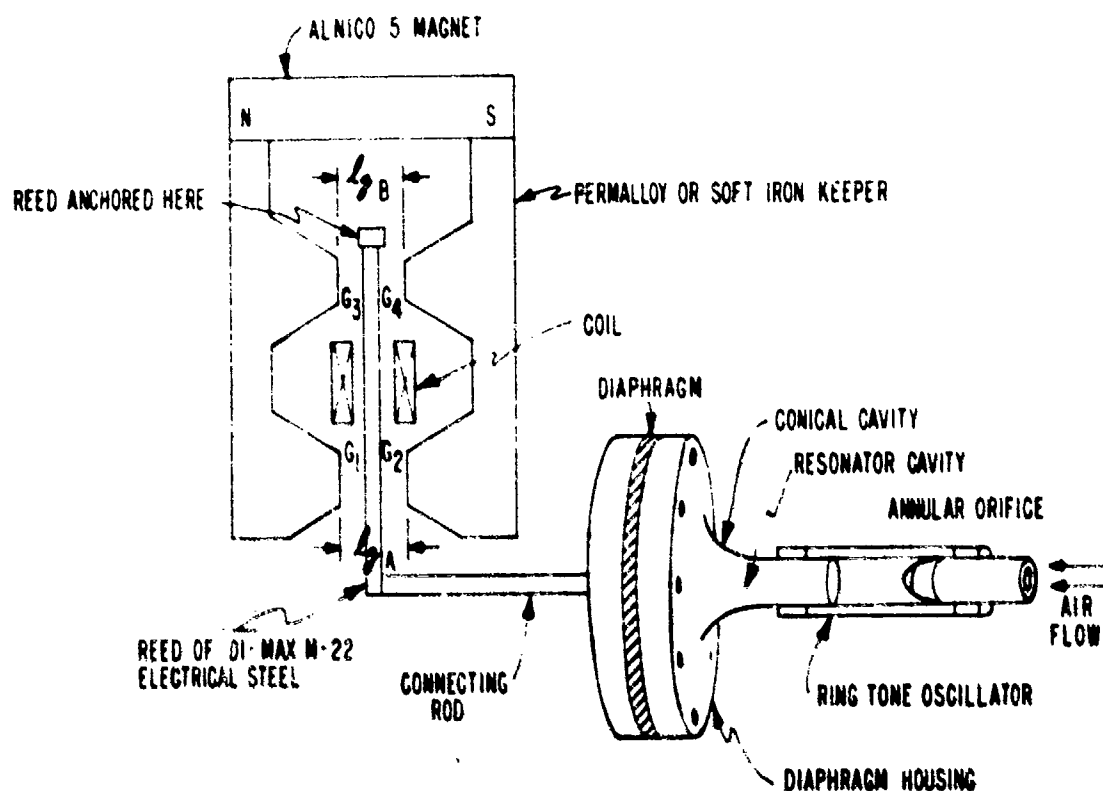


Fig. 1. Schematic View of Fluidic Generator with Reed Type Magnetic Transducer

---

1. Carl J. Campagnoulo, "The Fluidic Generator," NDL Technical Report-1328, September 1966.
2. Carl J. Campagnoulo, "Fluidic Power Generators for Ordnance Application," NDL Technical Report-1423, December 1968.
3. Carl J. Campagnoulo and Richard N. Gottron, "The Fluidic Generator: A New Electrical Power Source," 24th Annual Proceedings Power Sources Symposium, May 19-21, 1970.

As the projectile moves forward, air is forced through the annular orifice to excite the resonant cavity beyond. The oscillations of the cavity in turn cause the diaphragm to vibrate. This vibration is then transmitted to a permeable reed of Armco electrical steel. As can be seen from Fig. 1, when the reed is in its equilibrium position it is exactly midway between the pole pieces of both magnetic gaps and, therefore, carries no magnetic flux. The vibration of the reed, however, changes the relative lengths of gaps 1 and 2 and flux passes through the reed, alternating direction with the frequency of vibration. Gaps 3 and 4 are taken to remain constant and equal. The alternating flux through the reed induces an ac voltage in the coil around it and causes a current to flow in a circuit with a load resistance  $R_L$ . To optimize the design parameters we need an analysis of the magnetic circuit of the transducer. This will enable us to calculate the energy dissipated in  $R_L$  as a function of the gaps between pole pieces ( $P_i$ ), the reed thickness ( $t$ ), the reed displacement amplitude ( $a$ ), and the frequency of vibration of the reed ( $f$ ).

#### THE MAGNETIC CIRCUIT EQUATIONS

The magnetic circuit can be replaced by the analogous electric circuit as shown in Fig. 2, where the various electrical admittances have the values

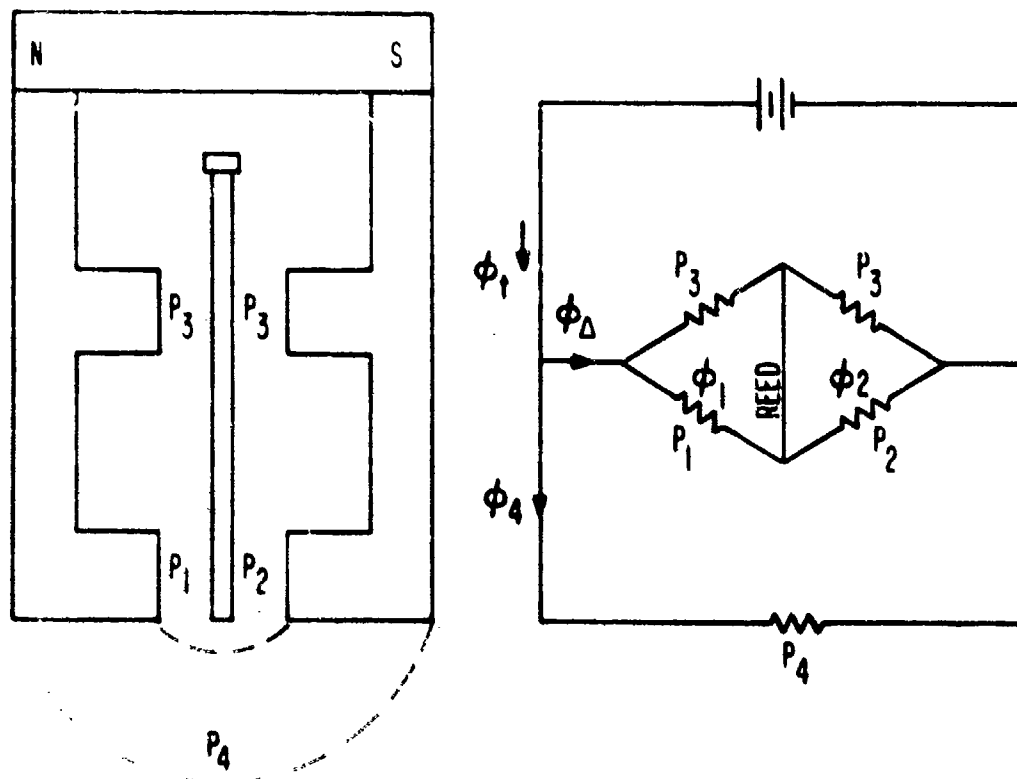


Fig. 2. Schematic Representation of the Magnetic Circuit and its Electrical Analogue

of the relevant magnetic permeances ( $P$ ) of the reed generator, and the magnitudes of the currents deduced will then be the same as those of the fluxes ( $\Phi$ ) carried in the corresponding branches of the magnetic circuit. The circuit analysis is straightforward:

$$\Phi_{\Delta} = \frac{P_{\Delta}}{P_4 + P_{\Delta}} \Phi_t \quad (1)$$

$$\Phi_1 = \frac{P_1}{P_1 + P_3} \Phi_{\Delta} \quad (2)$$

$$\Phi_2 = \frac{P_2}{P_2 + P_3} \Phi_{\Delta} \quad (3)$$

$$\Phi_R = \Phi_1 - \Phi_2 \quad (4)$$

Substituting (1), (2), and (3) in (4) yields

$$\Phi_R = \left( \frac{P_1}{P_1 + P_3} - \frac{P_2}{P_2 + P_3} \right) \frac{\Phi_t}{1 + \frac{P_4}{P_{\Delta}}} \quad (5)$$

$$\frac{1}{P_{\Delta}} = \frac{1}{P_1 + P_3} + \frac{1}{P_2 + P_3} \quad (6)$$

$$P_{\Delta} = \frac{(P_1 + P_3)(P_2 + P_3)}{P_1 + P_2 + 2P_3} \quad (7)$$

Substitution of (7) in (5) finally gives us:

$$\Phi_R = \Phi_t \left( \frac{P_1}{P_1 + P_3} - \frac{P_2}{P_2 + P_3} \right) \frac{1}{1 + \frac{P_4(P_1 + P_2 + 2P_3)}{(P_1 + P_3)(P_2 + P_3)}} \quad (8)$$

$$\Phi_R = \Phi_t \left( \frac{P_1}{P_1 + P_3} - \frac{P_2}{P_2 + P_3} \right) \left( \frac{(P_1 + P_3)(P_2 + P_3)}{(P_1 + P_3)(P_2 + P_3) + P_4(P_1 + P_2 + 2P_3)} \right) \quad (9)$$

$$\Phi_R = \Phi_t \frac{P_1(P_2 + P_3) - P_2(P_1 + P_3)}{(P_1 + P_3)(P_2 + P_3) + P_4(P_1 + P_2 + 2P_3)} \quad (10)$$

$$\Phi_R = \Phi_t \frac{P_3(P_1 - P_2)}{(P_1 + P_3)(P_2 + P_3) + P_4(P_1 + 2P_3 + P_2)} \quad (11)$$

## THE PERMEANCE CALCULATIONS

At this point it is necessary to obtain expressions for the various permeances  $P$  in terms of the reed displacement amplitude ( $a$ ) and the configurational parameters which can be conveniently varied, namely the two gap lengths  $i_{gA}$  and  $i_{gB}$ , and the reed thickness  $t$ . Since  $i_{gA}$  is always kept equal to  $i_{gB}$  we denote both gap lengths by  $i_g$ .

These permeances will be calculated by essentially the same techniques used in Ref. 4. These consist principally of approximating the actual flux paths by circular arcs and then applying the permeance formulae for these paths as listed in the standard text by Roters.<sup>5</sup> Suitable modifications of these general formulae must sometimes be made to deal with the peculiarities of a particular configuration. The actual arrangements for the prototype generator in both the isolated and in-shell conditions are shown in Figs. 3 and 4 respectively. The numerical values of the pertinent configurational dimensions are summarized in Table I.

The permeances associated with all of the flux paths which do not pass through the reed are collectively denoted by  $P_4$ . There are five such paths which are schematically illustrated in Fig. 5, and are calculated immediately below along with the other permeances illustrated in Fig. 5. All calculated permeances are in inches.

### (1) $P_{p4}$ (Fig. 5-A)

The flux path here is in the form of a parallel plate magnetic capacitor and the permeance is simply given by

$$P_{p4} = \frac{\text{Plate Area}}{\text{Plate Separation}} = \frac{A_p}{S} = \frac{(0.7)(0.365)}{0.395} = 0.647 \text{ in.} \quad (12)$$

$P_{p4}$  will be slightly modified by the presence of the reed, but since the reed is very thin compared to the separation of the keeper plates this modification is very small and will be neglected.

### (2) $P_{y4}$ (Fig. 5-B)

This is a standard permeance path for which the formula is

$$0.318 y \ln \left( 1 + \frac{2w}{s} \right) \quad (13)$$

where  $y$  is the common perimeter length of the keeper edges linked by the flux path. In the fluidic generator  $y \approx 2.2$  inches.  $w$  is the edge thickness .07" and  $s$  is the diameter of the smaller of the two semicircular boundaries of the flux path (.395"). Insertion of these values into Eq. (13) yields

4. H.A. Leupold, F. Rothwarf, C.G. Campagnola, J. Fine, and H. Lee, "Magnetic Circuit Design Studies for an Inductive Sensor," ECOM Technical Report-4158, October 1973.

5. H. Roters, Electromagnetic Devices, (John Wiley & Sons, Inc., 1941).

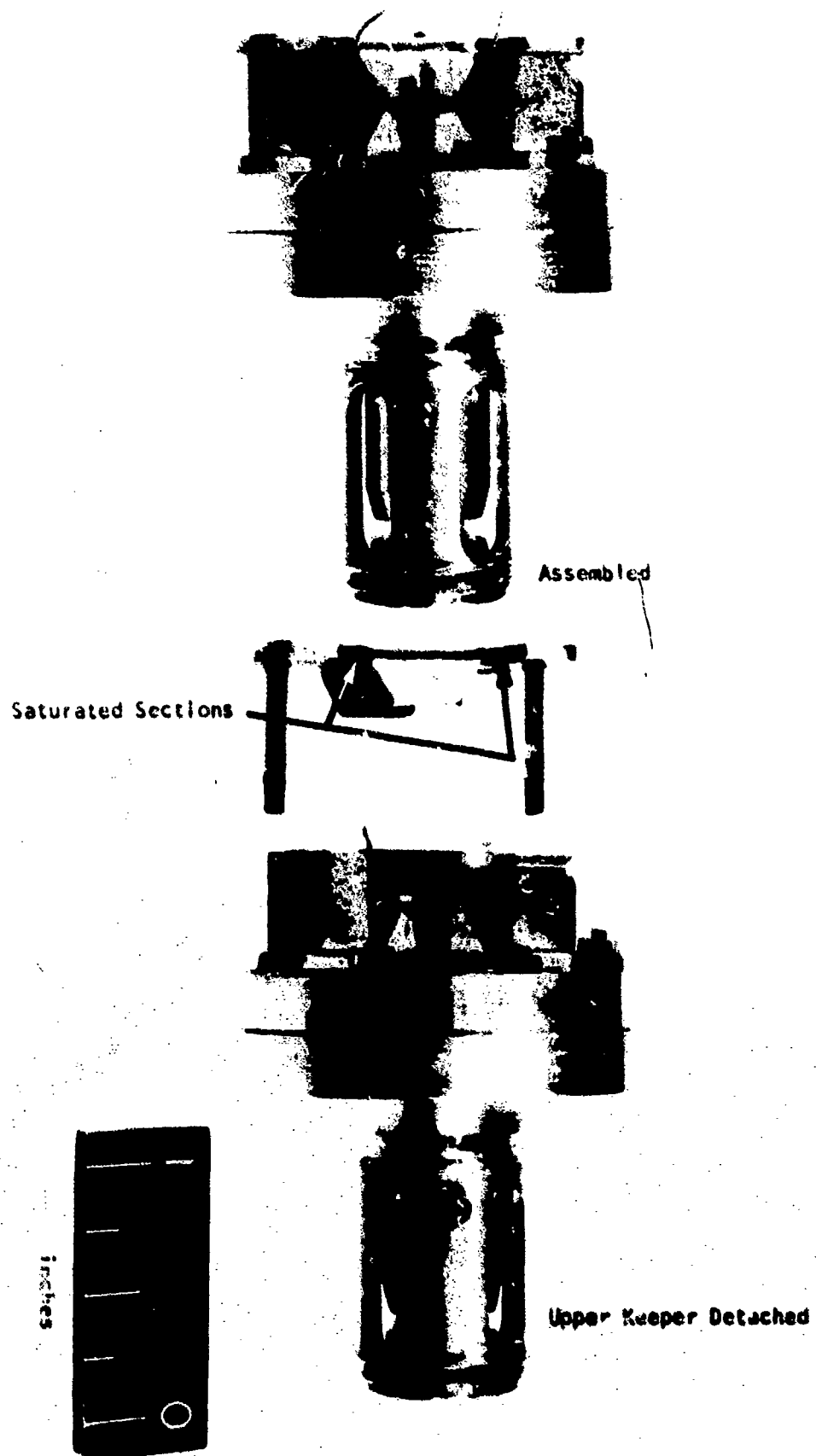
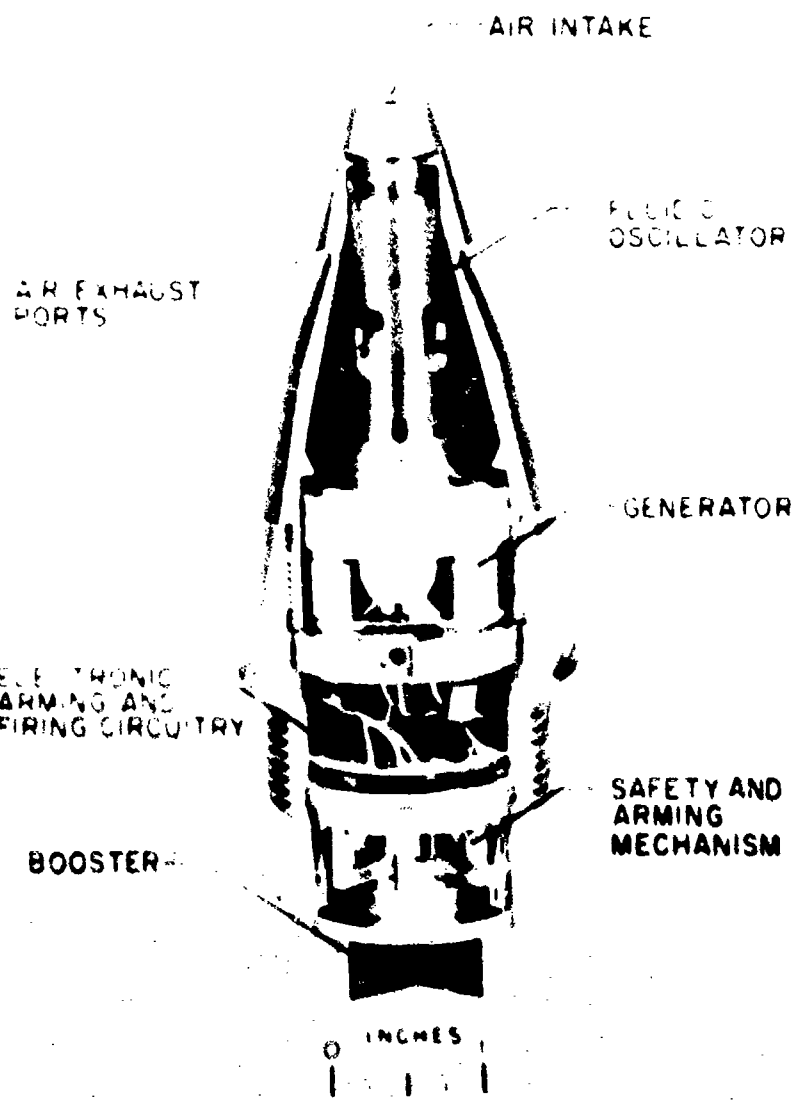


Fig. 3. Fluidic Generator.



## HDL HIGH PERFORMANCE PD FUZE FOR ARTILLERY AND MORTAR

Fig. 4. Sectional View of Fluidic Generator  
in Projectile Ogive

TABLE I  
Fixer Dimensions of Generator Configuration and Values of Critical Constants

<u>Fixer</u>	<u>Inches</u>	<u>cm</u>	<u>Magnet</u>	<u>Inches</u>	<u>cm</u>
Plate area for $P_{\mu_2}$ calculation	0.256 in <sup>2</sup>	1.65 cm <sup>2</sup>	Length	0.395	1.00
Plate separation	0.395	1.00	Cross-section area	0.337 in <sup>2</sup>	2.17 cm <sup>2</sup>
Thickness	0.070	0.178	Effective outer leakage perimeter	2.3	5.8
Width (narrowest)	0.360	0.914			
Perimeter (effective)	2.2	5.6			
Saturation flux density	16,000 gauss				
Resistivity $\rho$	45 $\mu\Omega$ cm				
Hysteresis constant $\eta$	0.0001				
<u>Reed</u>	<u>Inches</u>	<u>cm</u>	<u>Reed</u>	<u>Inches</u>	<u>cm</u>
Face thickness	0.070	0.178	Width	0.270	0.686
Face width	0.313	0.795	Effective length	0.500	1.27
Face perimeter	0.766	1.95	Thickness *	0.0320	0.0812
Face area	0.0219 in <sup>2</sup>	0.141 cm <sup>2</sup>	Projection beyond gap	0.150	0.381
Average width	0.475	1.21	Vibrational amplitude *	0.017	0.043
Height (inner)	0.150	0.381	Volume *	0.00432 in <sup>3</sup>	0.0706 cm <sup>3</sup>
Height (outer)	0.235	0.597	Saturation flux density $B_m$	19,900 gauss	
Gap length *	0.070	0.178	Resistivity $\rho$	50 $\mu\Omega$ cm	
			Hysteresis constant $\eta$	.002	
			Projection beyond pole pieces	0.15	0.38

\* Values are for sample calculations only. They are variable for computer calculated values in Table I (see Appendix II).

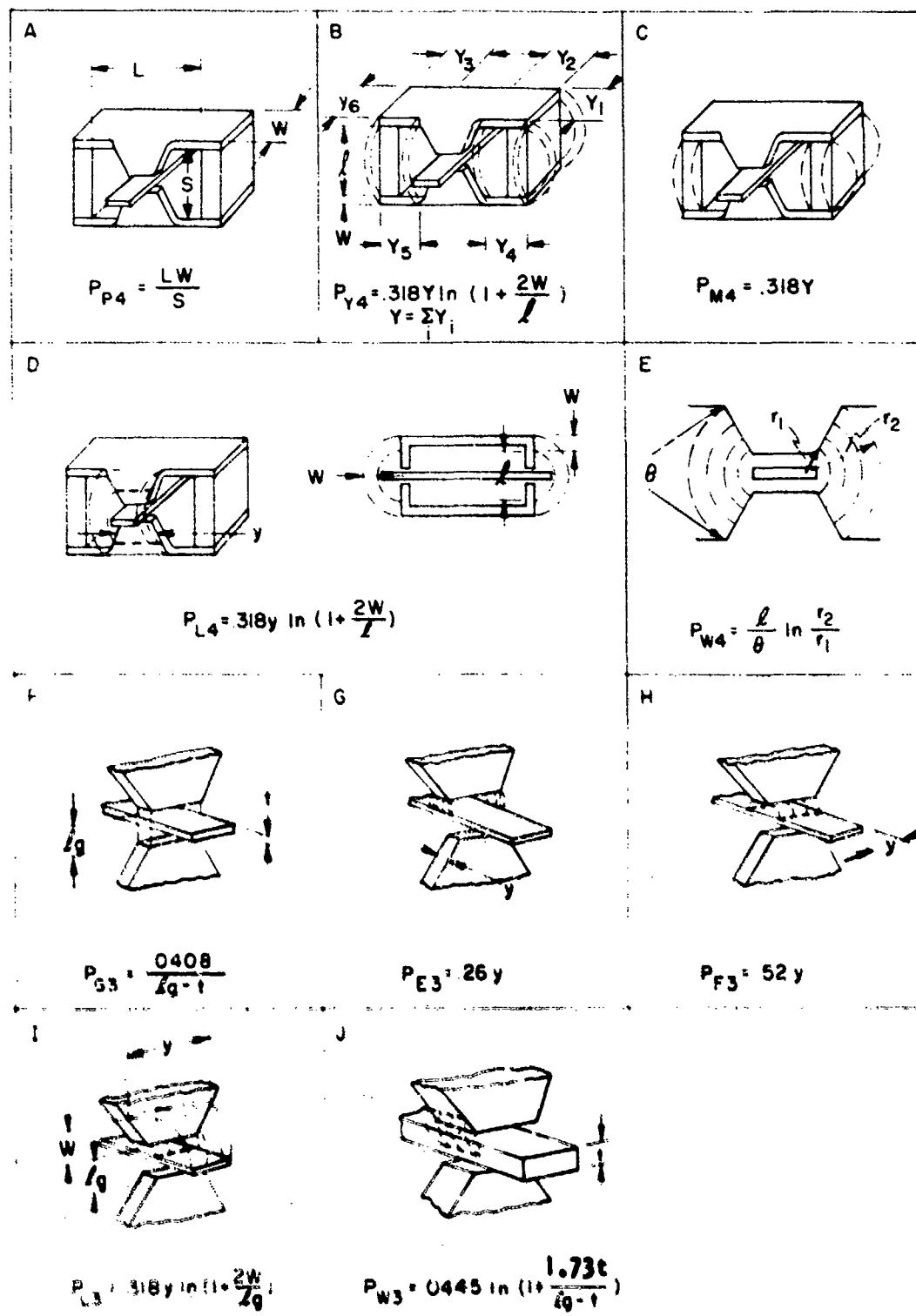


Fig. 5. Calculation of the Relevant Permeances

$$P_{M4} = .318 (2.2) \ln \left( 1 + \frac{2(0.07)}{.395} \right) = (.318)(2.2)(.303) = .212''$$

(3)  $P_{M4}$  (Fig. 5-C)

This is not a standard permeance but an expression for it can be derived as follows: Consider for the time being only that portion of the permeance path formed by the annular ring of width  $W$  as shown in Fig. 6. As we shall

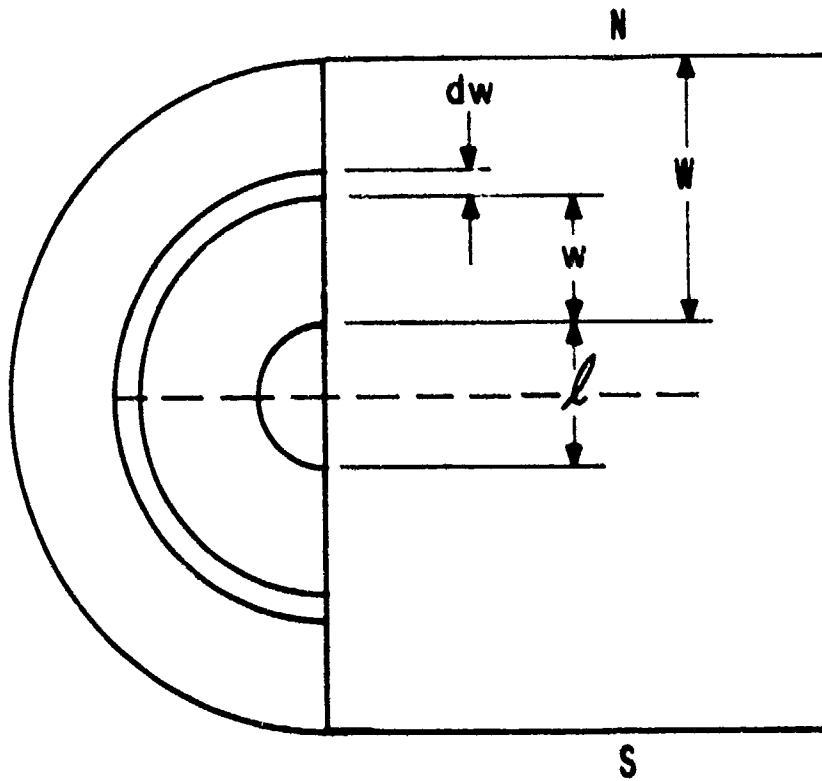


Fig. 6. Calculation of the Permeance  $P_{M4}$

see a simple extension of the resulting formula can then be used to determine the remaining permeance consisting of the semicircular region of diameter  $l$ . The permeance of a path such as the annular ring is of the same standard form as Eq. (13), i.e.

$$P = .318 y \ln \left( 1 + \frac{2W}{l} \right) \quad (14)$$

Similarly, the portion of the permeance within the annular ring of width  $w$  is

$$P = .318 y \ln \left( 1 + \frac{2w}{l} \right) \quad (15)$$

and the permeance of element  $dw$  is

$$dP = \frac{.318y \frac{2}{l} dw}{1 + \frac{2w}{l}} \quad (16)$$

However, since the flux lines are emanating from the sides of a magnet, the magnetomotive force driving an element such as  $dw$  is only a fraction of the full MMF of the magnet. Since this MMF is in direct proportion to the distance of the path terminals from the magnet center, this fraction is equal to

$$f = \frac{\frac{l}{2} + w}{\frac{l}{2} + W} \quad (17)$$

and the effective permeance of  $dP$  is reduced by the factor  $f$ , viz.,

$$dP_{\text{eff}} = f dP = .318y \frac{\left(\frac{l}{2} + w\right) \frac{2}{l}}{\left(\frac{l}{2} + W\right) \left(1 + \frac{2w}{l}\right)} dw$$

$$dP_{\text{eff}} = \frac{.318y}{\left(\frac{l}{2} + W\right)} \quad (18)$$

and the total permeance of the annular ring  $W$  is

$$P_{\text{eff}} = \frac{.318y}{W + \frac{l}{2}} \int_0^W dw = \frac{.318y W}{W + \frac{l}{2}} \quad (19)$$

To obtain the total effective permeance  $P_{M4}$  one needs only to set  $l = 0$  in the expression for  $P_{\text{eff}}$  and we are left with

$$P_{M4} = .318y \quad (20)$$

$y$  is just the perimeter of the magnet minus the length of the inner wall. The latter length is subtracted because it is rendered largely ineffective by competition from the flux paths of permeance  $P_{p4}$ . The effective  $y$  is somewhat awkward to estimate because of irregularities such as the screw slots cut into the magnet walls, but 2.3" seems a reasonable value for the two magnets together. Accordingly, our value for  $P_{M4}$  is

$$P_{M4} = (.318)(2.3) = .731"$$

#### (4) $P_{L4}$ (Fig. 5-D)

This again is a standard permeance of the form used in  $P_{p4}$ . There is one such path for the outside surface of each pole piece so we must multiply Eq. (13) by two. The flux lines emanating from the inner surfaces

go to the reed and hence contribute to  $P_1$ ,  $P_2$ , and  $P_3$  rather than to  $P_{L4}$ . For  $y$  we take the average width, (.475") of the effective portion of the trapezoidal outer surface of each pole piece.  $l$ , (.30") is twice the length of the reed projection beyond the gap as is clear from Fig. 5-D. As .235" is the height of the trapezoidal pole piece plus the gap from the pole face to reed, it also follows from Fig. 5-D that  $w = (.235 - .150) = .085"$ . Inserting these values in Eq. (13) yields

$$P_{L4} = 2(.318)(.475) \ln \left( 1 + \frac{2(.085)}{.300} \right)$$

$$P_{L4} = .302 \ln 1.57 = .136"$$

(5)  $P_{w4}$  (Fig. 5-E)

The formula for a path of this kind is

$$P = \frac{l}{\theta} \ln \frac{r_2}{r_1} \quad (21)$$

and since we have four such paths (2 for each pair of pole pieces)

$$P_{w4} = 4 \frac{l}{\theta} \ln \frac{r_2}{r_1} \quad (22)$$

$l$  is just the thickness of our pole pieces which is .070" and  $\theta$  is  $\frac{2}{3}\pi$  radians.  $r_2$  is the distance from the vertex of angle  $\theta$  to the larger base of the trapezoidal pole piece. Thus,  $r_2$  is equal to the length of the pole piece edge plus one-half the gap width divided by the sine of  $\frac{\pi}{3}$  radians. So since the pole piece edge is .2" long

$$r_2 = .2 + \frac{g}{2} \csc \frac{\pi}{3} = .2 + .577 \frac{g}{2} \quad (23)$$

$r_1$  is equal to  $\frac{g}{2} \csc \frac{\pi}{3}$  plus the distance along the pole piece edge from which the flux lines go to the edge of the reed. The latter distance is just one half the reed thickness ( $t$ ). So finally we have

$$r_1 = \frac{t}{2} + .577 \frac{g}{2} \quad (24)$$

and

$$P_{w4} = \frac{(4)(.070)(3)}{2\pi} \ln \frac{.2 + .577 \frac{g}{2}}{\frac{t}{2} + .577 \frac{g}{2}} \quad (25)$$

$$P_{w4} = .134 \ln \frac{.2 + 1.16 \frac{g}{2}}{t + 1.16 \frac{g}{2}} \quad (26)$$

(6)  $P_4$

We now have expressions for all of the components of the "leakage permeance"  $P_4$ , so  $P_4$  is given by:

$$\begin{aligned} P_4 &= P_{p4} + P_{y4} + P_{M4} + P_{L4} + P_{w4} \\ P_4 &= .647 + .212 + .731 + .136 + .134 \ln \frac{.4 + 1.16 \frac{L_g}{g}}{t + 1.16 \frac{L_g}{g}} \\ P_4 &= 1.72 + .134 \ln \frac{.4 + 1.16 \frac{L_g}{g}}{t + 1.16 \frac{L_g}{g}} \end{aligned} \quad (27)$$

If the gap is varied in the usual manner, i.e. by placing permalloy shims between the magnets and the permalloy keeper,  $P_{w4}$ ,  $P_{p4}$ , and  $P_{y4}$  will be slightly affected, but since the shim thicknesses are only of the order of 10 or 20 thousandths of an inch the change in these quantities will be negligible.

(7)  $P_{G3}$  (Fig. 5-F)

This is the permeance of the gap between the reed and either pole piece at the pinned end of the reed. The length of this gap  $L$  is given by

$$L = \frac{L_g}{2} - t \quad (28)$$

Since the widths of the pole piece (.313") and the reed .270" are not the same, we take an average (.291") in our determination of the gap's cross-sectional area. The pole face thickness is .070" so

$$P_{G3} = \frac{\text{Area}}{L} = \frac{2(.070)(.291)}{\frac{L_g}{2} - t} \quad (29)$$

$$P_{G3} = \frac{.0408}{\frac{L_g}{2} - t} \quad (30)$$

If the gap sizes are varied by machining the pole faces the constant in this formula will change due to the alteration in cross-sectional area of the pole faces.

(8)  $P_{E3}$  (Fig. 5-G)

$P_{E3}$  is the permeance of the path extending from the edges of the reed to the pole face edges parallel to the former. The standard expression for this type of permeance path is

$$P = .26y \quad (31)$$

where  $y$  is the edge length which here is the thickness of the pole piece (.070") so

$$P = (.26)(.070) = .0182" \quad (32)$$

Since we have two such edges the total permeance is

$$P_{E3} = 2P = (2)(.0182) = .0364" \quad (33)$$

(9)  $P_{F3}$  (Fig. 5-H)

These are the paths from the edges of the pole pieces to the flat portion of the reed. These are standard forms whose permeances are given by

$$P = .52y = .52(.291) \quad (34)$$

Since there are two paths we have

$$P_{F3} = 2P = 2(.52)(.291) = .303" \quad (35)$$

(10)  $P_{L3}$  (Fig. 5-I)

These permeances involve the paths between the walls of the pole pieces and the wide faces of the reed. The general expressions are the same as those for  $P_{L4}$  except for a factor of 2 to take into account that the flux lines here are quarter circles rather than semicircles as in  $P_{L4}$ . The gap length  $l$  used in the formula must be taken as twice the separation between the reed and the pole piece, i.e.,

$$l = 2 \left( \frac{l_g - t}{2} \right) = l_g - t.$$

The quantity  $w_i$  for the inner flux path is just the altitude of the trapezoidal pole piece which is .15". For the effective  $y$  one chooses an average of the reed width (.270") and the width of the trapezoid midway between its bases (.406"). This results in a value  $y = .338"$ .

The outer path must be treated slightly differently because the reed projects only .15" beyond the gap edge. Accordingly,  $w_0$  is just taken as

$$w_0 = .15 - \frac{(l_g - t)}{2} \quad (36)$$

and the average value  $y$  is also slightly altered.

As is seen in Fig. 7 the flux lines from the reed extend only up to line AB which is .15" above the top surface of the reed. The average width of the flux-emitting region of the pole face is then

$$y_F = \frac{AB + .313}{2} \quad (37)$$

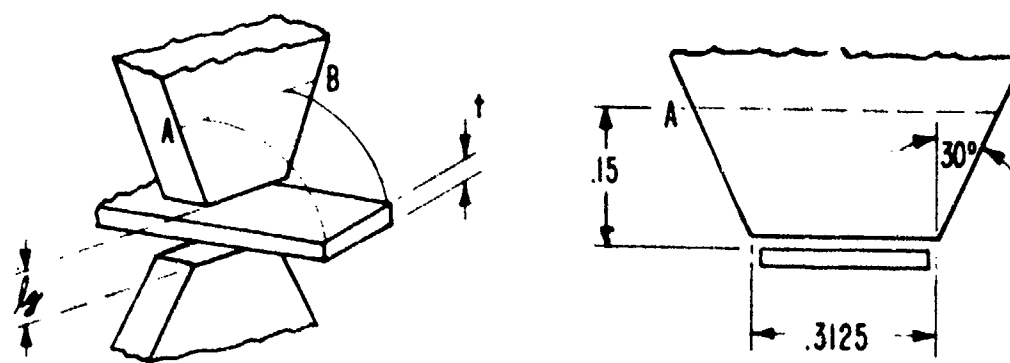


Fig. 7. Determination of the width  $y_F$  in the formula for Permeance  $P_{L3}$

and

$$y_0 = \frac{y_F + y_R}{2} \quad (38)$$

where  $y_R = .270$  is the reed width.

$$AB = .313 + 2 \left( .15 - \left( \frac{L_g - t}{2} \right) \right) \tan 30^\circ \quad (39)$$

$$AB = .313 + (.30 - (L_g - t)) .577$$

$$AB = .486 - .577 (L_g - t) \quad (40)$$

$$y_F = \frac{.486 - .577 (L_g - t) + .313}{2} = .399 - .289 (L_g - t) \quad (41)$$

$$y_0 = \frac{.399 - .289 (L_g - t) + .270}{2} \quad (42)$$

$$y_0 = .335 - .144 (L_g - t) \quad (43)$$

Substituting these values in the general expression yields

$$P_{L3} = 2(.318)(.338) \ln \left( 1 + \frac{2(.15)}{L_g - t} \right) + 2(.318)[.335 - .144 (L_g - t)] \ln \left( 1 + \frac{2 \left( .15 - \frac{L_g - t}{2} \right)}{L_g - t} \right) \quad (44)$$

$$P_{L3} = .215 \ln \left( 1 + \frac{.30}{L_g - t} \right) + (.213 - .0916 (L_g - t)) \ln \left( 1 + \frac{.30 - (L_g - t)}{L_g - t} \right) \quad (45)$$

$$P_{L3} = .215 \ln \left( 1 + \frac{.30}{L_g - t} \right) + (.213 - .0916 (L_g - t)) \ln \left( \frac{.30}{L_g - t} \right) \quad (46)$$

(11)  $P_{w3}$  (Fig. 5-J)

If the arrow side face of the reed were coplanar with the narrow face of the wide piece as indicated by the dashed line in Fig. 5-J, the expression for permeance  $P_{w3}$  would be the often used standard form

$$P_{w3} = .318y \ln \left( 1 + \frac{2w}{L} \right) \quad (47)$$

Although it is possible to correct for the fact that the actual flux lines are shorter than in this ideal case, the correction would be very small, and since the total permeance  $P_{w3}$  is itself so small as to barely affect the calculations with one significant figure, this correction is completely

negligible and will not be made here. So  $w$  is taken as  $\frac{t}{2}$ ,  $L = \frac{L_g - t}{2 \cos 30^\circ}$ .

$y = .070$ , and we precede the expression with the factor 2 because there are two paths of this type

$$P_{w3} = 2(.318)(.070) \ln \left( 1 + \frac{2t \cos 30^\circ}{L_g - t} \right) \quad (48)$$

$$P_{w3} = .0445 \ln \left( 1 + \frac{1.73t}{L_g - t} \right) \quad (49)$$

(12)  $P_{G1}$  and  $P_{G2}$

These permeances are of the same form as  $P_{G3}$  with allowance made for the spacing changes due to the displacement of the reed. When the reed is at equilibrium, that is, at zero displacement,  $P_{G1} = P_{G2} = P_{G3}$ . Since we are interested in the maximum and minimum values of  $P_{G1}$  and  $P_{G2}$ , we write them in terms of the displacement amplitude ( $a$ ) of the reed.

$$P_{G1}^{\max} = P_{G2}^{\max} = \frac{.0408}{L_g - t - 2a} \quad (50)$$

$$P_{G1}^{\min} = P_{G2}^{\min} = \frac{.0408}{L_g - t + 2a} \quad (51)$$

where  $P_{G1}$  is a maximum when  $P_{G2}$  is a minimum and vice versa.

(13)  $P_{E1}$

$$P_{E1} = P_{E3} = .0364'' \quad (52)$$

(14)  $P_{F1}$

$$P_{F1} = P_{F3} = .303'' \quad (53)$$

(15)  $P_{w1}$  and  $P_{w2}$

$P_{w1}$  is of the same form as  $P_{w3}$  when the reed is in equilibrium. When  $P_{w1}$  is a maximum,  $t = (l_g - t)$  must be replaced by  $(l_g - t - 2a)$  and by  $(l_g - t + 2a)$  when  $P_{w1}$  is a minimum. The same holds for  $P_{w2}$ . Thus we have

$$P_{w1}^{\max} = P_{w2}^{\max} = .0445 \ln \left( 1 + \frac{1.73t}{l_g - t - 2a} \right) \quad (54)$$

$$P_{w1}^{\min} = P_{w2}^{\min} = .0445 \ln \left( 1 + \frac{1.73t}{l_g - t + 2a} \right) \quad (55)$$

(16)  $P_{L1}$  and  $P_{L2}$

The term in  $P_{L1}$  arising from the inner flux path is the same as the corresponding term in  $P_{L3}$  except that again the quantity  $(l_g - t)$  is replaced by  $(l_g - t - 2a)$  or  $(l_g - t + 2a)$  to obtain  $P_{L1}^{\max}$  and  $P_{L1}^{\min}$ , respectively.

The term arising from the outer flux path is similarly derived from the corresponding term in  $P_{L3}$  by the same substitution but an additional alteration is necessary. The portion of the reed projecting beyond the limits of the gap is triangular rather than rectangular as is the projection at the anchored end of the reed. For this reason the flux lines emanating from the walls of the pole piece have only one half the reed area in which to terminate. To take this into account it seems reasonable to substitute in the expression for  $y_g$ , one half of the reed width for the full reed width. Thus, in Eq. (42) the value of .270 is replaced by .135. After all these adjustments are made the expression for  $P_{L1}$  and  $P_{L2}$  becomes

$$P_{L1}^{\min} = P_{L2}^{\min} = .215 \ln \left( 1 + \frac{.30}{l_g - t \mp 2a} \right) + .170 - .0916 (l_g - t \mp 2a) \ln \frac{.30}{l_g - t \mp 2a} \quad (56)$$

There are other permeances associated with flux paths going from corner to corner, edge to corner and face to corner. In this problem, these are not of standard form and are very difficult to estimate. They tend however, to be small compared to most of the calculated permeances, and the labor of any attempt to estimate them would not be justified by the precision attainable by our computational techniques.

## CALCULATIONS OF GAP FLUX DENSITIES IN THE ABSENCE OF A REED

We now have expressions for all of the permeances relevant to the desired power calculations. Before a sample calculation for particular values of  $l_g$ ,  $t$  and  $a$  are made, it would be instructive to calculate the field in the gaps when the reed is not present. Since a measured field value exists for a gap width of .060, a comparison with the result of our calculation would give an indication as to the general efficacy of the computational methods used. To do this we need the permeance  $P_{G4}$  which is given by:

$$P_{G4} = \frac{(2)(\text{Area Pole Faces})}{\text{Gap Length}} = \frac{(2)(.0219)}{.06} = .730'' \quad (57)$$

We now also have the permeances  $P_{E4}$  between the corresponding edges of the pole faces and  $P_{C4}$  between the corresponding corners on either side of the gap.  $P_{E4}$  is given by the usual formula  $P_{E4} = 2(.26)y$ , where  $y$  is the perimeter of a pole face and the factor of 2 enters because there are two gaps.  $P_{C4}$  is given by  $(8)(.077)l_g$ , where the factor 8 occurs because there are four corner-to-corner permeances for each of the two gaps. Therefore,  $P_{C4}$  is given by

$$P_{C4} = (8)(.077)(.060) = .0369'' \quad (58)$$

$P_{E4} = (.52)(.766) = .398$ .  $P_{p4}$ ,  $P_{y4}$  and  $P_{m4}$  are the same as when the reed is present. We, therefore, need only to find the new values of  $P_{w4}$  and  $P_{l4}$ .  $P_{w4}$  is given by Eq. (26) with  $t$  set equal to zero. Thus

$$P_{w4} = .134 \ln \frac{s_4 + (1.16)(.06)}{1.16(.06)} = .134 \ln 6.75$$

$$P_{w4} = (.134)(1.91) = .256'' \quad (59)$$

The contributions of the two outer surfaces to  $P_{l4}$  are given by the same formula as when the reed is present, but now  $l = l_g = .06$  and

$$\bar{y} = \frac{s_4 + s_{13}}{2} = .406. \text{ So these contributions}$$

$$P_{l4}^0 = 2(.318)(.406) \ln \left( 1 + \frac{2(.2)}{.06} \right) = .258 \ln 7.67$$

$$P_{l4}^0 = (.258)(2.04) = .526'' \quad (60)$$

In the absence of the reed the inner surfaces also contribute. The longest semicircular arc of this path, however, must be no longer than the distance  $d$  as shown in Fig. 8, so

$$\pi \left( \frac{d}{2} + w \right) = d \quad (61)$$

$$w = \frac{d}{\pi} - \frac{d}{2} \quad (62)$$

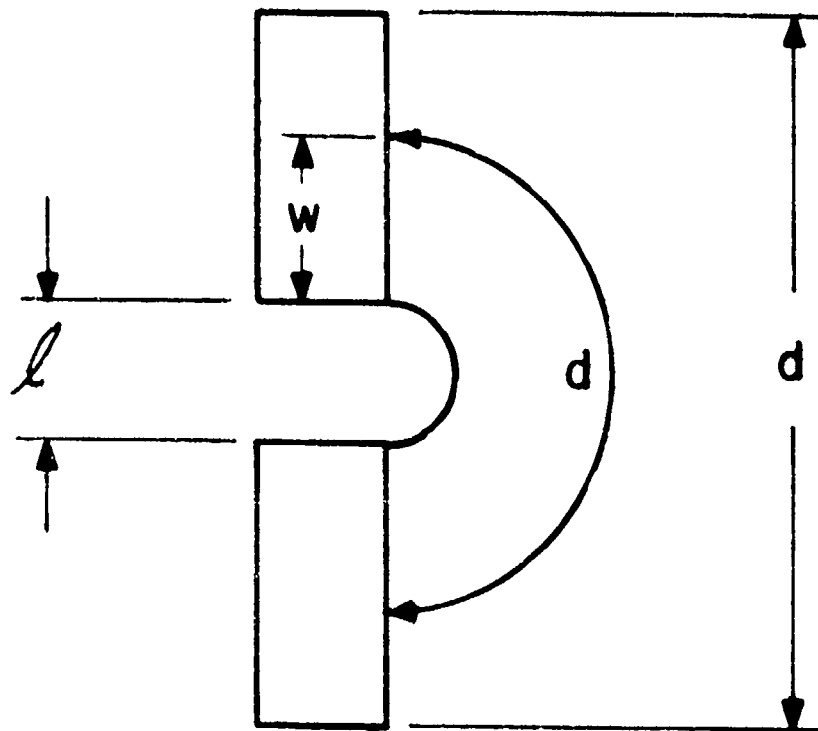


Fig. 8. Determination of the Inner Flux Paths Comprising Permeance  $P_{M4}$

$$w = \frac{.395}{3.14} - \frac{.060}{2}$$

$$w = .126 - .030 = .0958"$$

and

$$\bar{y} = \frac{2(.313) + (2)(.0958) \tan 30^\circ}{2} = .313 + .055 = .368" \quad (63)$$

Thus

$$P_{L4}^1 = 2(.318)(.368) \ln \left( 1 + \frac{2(.0958)}{.06} \right) = .234 \ln (4.03) = .325 \quad (64)$$

$$P_{L4} = P_{L4}^1 + P_{L4}^0 = .325 + .526 = .851"$$

Our total permeance  $P_4$  in the absence of a reed is then

$$P_4 = P_{G4} + P_{P4} + P_{y4} + P_{M4} + P_{w4} + P_{L4} + P_{E4} + P_{c4} \quad (65)$$

$$P_4 = .730 + .647 + .212 + .731 + .256 + .851 + .398 + .037$$

$$P_4 = 3.86 \quad (66)$$

In this case  $P_4$  is our total permeance  $P_t$  and from it we can obtain our load line slope

$$\frac{B}{H} = \frac{L}{A} P_t = \frac{(.395)}{(.337)} \frac{(3.86)}{1} = 4.52 \quad (67)$$

where  $L = .395$  in and  $A = .337$  in<sup>2</sup>. And from the intersection of the Alnico 5 demagnetization curve with the load line  $B/H = 4.52$  in Fig. 9 we obtain

$$\bar{B}_{mag} = 2670 \text{ gauss} \quad (68)$$

Since the magnetic configuration is of irregular shape,  $B$  is not perfectly uniform over the entire magnet, therefore,  $B_{mag}$  represents an effective average flux density. So the total flux output of the magnet is

$$\Phi_t = \bar{B}_{mag} A_{mag} = (2670)(2.17) = 5790 \text{ Maxwells} \quad (69)$$

The flux in one gap  $\Phi_G$  is given by

$$\Phi_G = \frac{P_{G4}}{2P_t} \Phi_t = \frac{.730}{2(3.86)} 5790 = 547 \text{ Maxwells} \quad (70)$$

and

$$B_G = \frac{\Phi_G}{A_G} = \frac{547}{.141} = 3880 \text{ gauss} \quad (71)$$

This value is about 29% higher than the measured value of 3000 gauss which is satisfactory agreement considering the various approximations made in the course of the calculations. One must also keep in mind that such comparisons should not be taken too seriously. The calculated  $B_G$  represents an average flux density obtained by dividing the total flux emanating from a pole face by the area of that pole face. The measured  $B_G$  can represent either a much more localized value of  $B_G$  or an average that includes fluxes not even associated with the gap, depending on the type, positioning and size of the probe used. The wider the gap compared to the pole face dimensions, the more difficult it is to obtain a meaningful measured value of  $B_G$ . Considering these limitations, we conclude that the general computational procedure yields reasonable agreement with the measured results, and that its judicious application to the determination of expected power outputs should not lead us too far astray.

#### SAMPLE CALCULATION FOR POWER OUTPUT IN THE LOAD RESISTANCE $R_L$

We will now perform a sample calculation for the most efficient configuration measured thus far. The relevant parameters for this arrangement are:  $L_g = .070"$ ,  $t = .032"$ ,  $a = .017"$ .

We will first calculate  $P_4$ . We need only the components,  $P_{W4}$  and  $P_{L4}$ . Using Eq. (26) we obtain

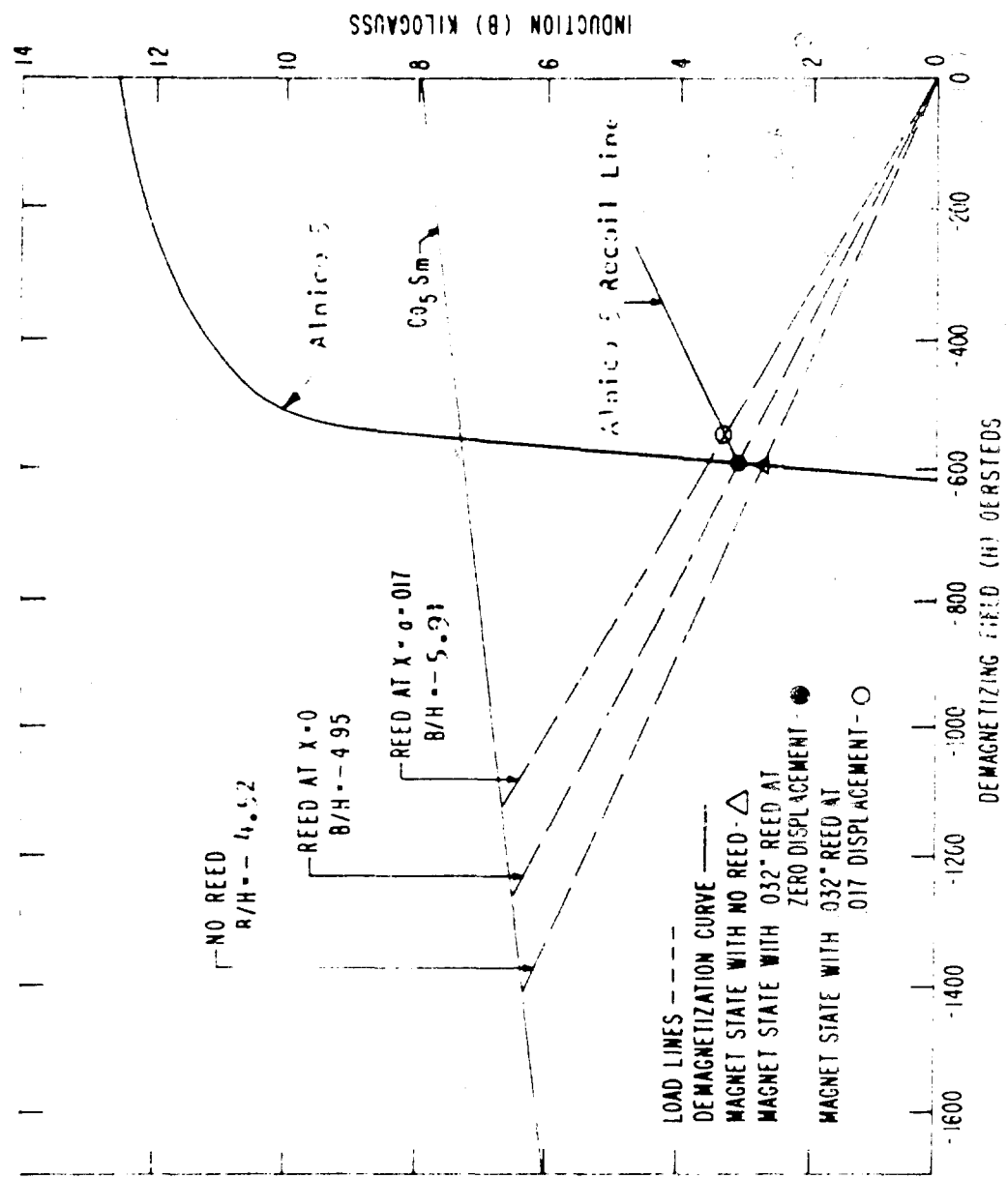


FIG. 9 DETERMINATION OF B FOR A FLUIDIC GENERATOR WITH A .070 " GAP LENGTH.

$$P_{w4} = .134 \ln \frac{.4 + 1.16 \ell_g}{t + 1.16 \ell_g} = .134 \ln \frac{.4 + (1.16)(.07)}{.032 + (1.16)(.07)}$$

$$P_{w4} = .134 \ln 4.26 = .134(1.45) = .194'' \quad (72)$$

The appropriate  $P_{L4}$  has already been calculated on page 11 and found to be .136. The other components of  $P_4$  are the same as were used to calculate the gap fields except that now there is no  $P_{G4}$ ,  $P_{E4}$  or  $P_{C4}$ . Thus

$$P_4 = P_{p4} + P_{y4} + P_{M4} + P_{L4} + P_{w4} \quad (73)$$

$$P_4 = .647 + .212 + .731 + .136 + .194$$

$$P_4 = 1.92'' \quad (74)$$

$P_3$  has five components

$$P_{G3} = \frac{.0408}{.070 - .032} = \frac{.0408}{.038} = 1.07'' \quad (75)$$

$$P_{E3} = .0364'' \quad (76)$$

$$P_{F3} = .303'' \quad (77)$$

$$P_{L3} = .215 \ln \left( 1 + \frac{.30}{\ell_g - t} \right) + (.213 - .0916 (\ell_g - t)) \ln \left( \frac{.30}{(\ell_g - t)} \right) \quad (78)$$

$$P_{L3} = .215 \ln \left( 1 + \frac{.30}{.038} \right) + (.213 - .0916(.038)) \ln \left( \frac{.30}{.038} \right)$$

$$P_{L3} = .215 \ln 8.90 + (.213 - .0916) \ln 7.90 = (.215)(2.19) + (2.09)(2.07)$$

$$P_{L3} = .470 + .432''$$

$$P_{L3} = .902'' \quad (79)$$

$$P_{w3} = .0445 \ln \left( 1 + \frac{1.73t}{\ell_g} \right) = .0445 \ln \left( 1 + \frac{(1.73)(.032)}{.038} \right) \quad (80)$$

$$P_{w3} = .0445 \ln (2.46) = (.0445)(.900) = .0400'' \quad (81)$$

$$P_3 = 1.07 + .0364 + .303 + .902 + .0400$$

$$\underline{\underline{P_3 = 2.35''}} \quad (82)$$

$P_1$  and  $P_2$ , when the reed is at its equilibrium position, are obtained by substituting  $a = 0$  in the expression for the components of  $P_1$  and  $P_2$  and then adding these components. This procedure yields  $P_1 = P_2 = 2.27''$ . We need to find  $P_t^E$ , that is, the total permeance at equilibrium to locate the point on the Alnico 5 demagnetization curve at which the recoil line begins. (Point E in Fig. 9)

$$P_t^E = P_4 + \frac{3}{2} + \frac{P_1}{2} = 4.23 \quad (83)$$

$$\left(\frac{B}{H}\right)_E = - \frac{L}{A} P_t^E = - (1.17)(4.23) = - 4.95 \quad (84)$$

$$B_M = 2950 \text{ gauss (from Fig. 9)} \quad (85)$$

$$H = - \frac{2950}{4.95} = - 596 \text{ Oe} \quad (86)$$

The slope of recoil lines for Alnico 5 is 4.3 so the equation of the recoil line is

$$B = 4.3H + B_0 \quad (87)$$

$$2950 = (4.3)(-596) + B_0$$

$$2950 + (4.3)(596) = B_0$$

$$2950 + 2560 = B_0$$

$$5510 = B_0 \quad (88)$$

So we have for our recoil line

$$B = 4.3H + 5510 \text{ gauss} \quad (89)$$

We now need only  $P_1$  and  $P_2$  to complete our analysis. Using Eqs. (50) and (51) we have

$$\frac{P_{G1}^{\max}}{P_{G2}^{\max}} = \frac{P_{G1}^{\max}}{P_{G2}^{\max}} = \frac{.0408}{L_g - t - 2a} = \frac{.0408}{.070 - .032 - 2(.017)} = \frac{.0408}{.004} \quad (90)$$

$$\frac{P_{G1}^{\max}}{P_{G2}^{\max}} = \frac{P_{G1}^{\max}}{P_{G2}^{\max}} = 10.2'' \quad (91)$$

$$\frac{P_{G2}^{\min}}{P_{G1}^{\min}} = \frac{P_{G2}^{\min}}{P_{G1}^{\min}} = \frac{.0408}{L_g - t + 2a} = \frac{.0408}{.070 - .032 + .034} = \frac{.0408}{.072} = .566'' \quad (92)$$

From (33) and (35) respectively, we have

$$P_{E1} = P_{E2} = .0364'' \quad (93)$$

$$P_{F1} = P_{F2} = .303" \quad (94)$$

From (54)

$$\begin{aligned} P_{w1}^{\max} &= .0445 \ln \left( 1 + \frac{1.73t}{L_g - t + 2a} \right) = .0445 \ln \left( 1 + \frac{(1.73)(.032)}{.070 - .032 + 2(.017)} \right) \\ P_{w2}^{\min} & \\ P_{w1}^{\max} &= .0445 \ln \left( 1 + \frac{0.0554}{.004} \right) = (.0445) \ln 14.85 \end{aligned}$$

$$P_{w1}^{\max} = (.0445)(2.70) = .120 \quad (95)$$

$$P_{w2}^{\min} = .0445 \ln \left( 1 + \frac{0.0554}{.072} \right) = .0445 \ln 1.77$$

$$P_{w2}^{\min} = (.0445)(.57) = .0254 \quad (96)$$

From (56)

$$P_{L1}^{\max} = .215 \ln \left( 1 + \frac{.30}{.004} \right) + [.170 - (.0916)(.004)] \ln \left( \frac{.30}{.004} \right)$$

$$P_{L1}^{\max} = .215 \ln 76 + .170 \ln 75 = (.215)(4.33) + (.170)(4.32)$$

$$P_{L1}^{\max} = .931 + .734 = 1.66 \quad (97)$$

Similarly

$$P_{L2}^{\min} = .215 \ln \left( 1 + \frac{.30}{.072} \right) + [.170 - (.0916)(.072)] \ln \left( \frac{.30}{.072} \right)$$

$$P_{L2}^{\min} = .215 \ln 5.17 + .163 \ln 4.17 = .215(1.64) + (.163)(1.43)$$

$$P_{L2}^{\min} = .353 + .233 = .586" \quad (98)$$

Finally, we have for  $P_1^{\max}$  and  $P_2^{\min}$

$$P_1^{\max} = 10.2 + .036 + .303 + .120 + 1.663$$

$$P_1^{\max} = 12.32 \quad (99)$$

$$P_2^{\min} = .566 + .036 + .303 + .025 + .586$$

$$P_2^{\min} = 1.52 \text{ in} \quad (100)$$

$$P_t^{\max} = P_4 + \frac{(P_1^{\max} + P_3) (P_2^{\min} + P_3)}{P_1^{\max} + P_2^{\min} + 2P_3} \quad (101)$$

$$P_t^{\max} = 1.92 + \frac{(12.32 + 2.35)(1.52 + 2.35)}{12.32 + 2.35 + 1.52 + 2.35}$$

$$P_t^{\max} = 1.92 + \frac{(14.67)(3.87)}{18.5} = 4.98 \text{ in} \quad (102)$$

$$\left(\frac{B}{H}\right)^{\max} = - \frac{i}{A} P_t^{\max} = - (1.17)(4.98) = - 5.83 \quad (103)$$

From (89)

$$B^{\max} = 4.3H + 5510$$

$$B^{\max} = \frac{5510}{1 + \frac{4.3}{5.83}} = \frac{5510}{1.73} = 3170 \text{ gauss} \quad (104)$$

$$\Phi_t^{\max} = B^{\max} A_{\text{magnet}} = (3170)(2.18) = 6880 \text{ Maxwells} \quad (105)$$

Substituting all of our calculated permeance values and  $\Phi_t^{\max} = 6880$  in Eq. (11) yields for the amount of flux carried by the reed

$$\Phi_R^{\max} = 6880 \frac{2.35(12.32 - 1.52)}{(14.7)(3.87) + (1.92)(18.5)}$$

$$\Phi_R^{\max} = \frac{(6880)(2.35)(10.8)}{92.4} = 1890 \text{ Maxwells} \quad (106)$$

The induced voltage amplitude is then given by

$$V^{\max} = \frac{N_L \Phi_R^{\max}}{10^8} \quad (107)$$

where  $\omega$  is the angular frequency of vibration of the reed, which in this case is  $2\pi(1500)$  and  $N = 1500$  is the number of turns in the coil.

$$V^{\max} = \frac{(1500)(2\pi)(1500)(1890)}{10^8} = 267 \text{ volts} \quad (108)$$

Attached to the coil is a 600- $\Omega$  load resistor and the resistance of the coil is 600  $\Omega$  as well. The inductance of the coil with a .017" reed is about 23 henrys. To find the power dissipated in the load, we need the total impedance  $Z$  of the circuit.

$$Z^2 = R^2 + X_L^2 = (1200)^2 + X_L^2 \quad (109)$$

The inductive reactance  $X_L$  is just

$$X_L = 2\pi f L = \frac{(6.28)(1500)(23)}{1000} = 217 \Omega \quad (110)$$

$$Z^2 = (1200)^2 + (217)^2 = 1.49 \times 10^6 \quad (111)$$

$$Z = 1220 \Omega \quad (112)$$

The root mean square current  $\bar{I}$  is given by  $\bar{I} = \frac{I_{\max}}{\sqrt{2}} = \frac{V_{\max}}{Z/2}$  and the power dissipated in the load  $P_L$  is then

$$P_L = \bar{I}^2 R_L = \frac{V_{\max}^2 R_L}{2Z^2} = \frac{(267)(267)(600)}{(2)(1220)(1220)} = 14.4 \text{ watts} \quad (113)$$

The actual power measured, however, was only 5 watts. The foregoing calculations were made on the assumption that the reed had infinite permeance. The electrical steel of which the reed is composed saturates at 19,900 gauss and its cross-section area is

$$A = (.27 \times .032 \times 2.54 \times 2.54) \text{ cm}^2 \quad (114)$$

Therefore, the maximum amount of flux it can carry is

$$\Phi_s = (19,900)(.27)(.032)(2.54)(2.54) = 1110 \text{ Maxwells} \quad (115)$$

and if, as was shown, 1890 Maxwells in the reed would yield 14.4 watts then the maximum allowable flux of 1110 Maxwells would give us

$$P_s = \sqrt{\frac{1110}{1890}}^2 \cdot 14.4 = 4.97 \text{ watts which is almost exactly the power observed.}$$

It, therefore, appears that to utilize the full flux output of the magnets used, the reed thickness must be increased by about 70%. Whether this can be done without drastically affecting the vibrational response to the oscillator is a mechanical problem beyond the scope of this study.<sup>3</sup> It is clear, however, that increased output with the present configuration depends largely upon increasing the flux carrying capability of the reed. If, on the other

---

3. Carl J. Campagnulo and Richard N. Gottron, "The Fluidic Generator: A New Electrical Power Source," 24th Annual Proceedings Power Sources Symposium, May 19-21, 1970.

hand, the present output of 5 watts is satisfactory, it can be attained with considerably less magnetic material since with the present arrangement 70% more flux is available than can be profitably used. Of course, if the reed thickness is increased, the gaps must be lengthened by an appropriate amount to keep the load line of the magnets the same and to maintain reasonable space in which the reed can oscillate. Also the expected power output would be altered slightly since the inductance of the coil is a function of reed thickness. This effect, however, would not be significant.

Parts of the keeper may also be saturated under the given operating conditions. The cross sections which would saturate first are the ones indicated in Fig. 3. Under the given conditions, the flux that must be carried by the narrowest sections of the keeper is given by

$$\Phi_s = \frac{\Phi_{\max}}{2} \frac{p_{\max}^{\max} - p_{\max}^{\min} - p_{\max}^{\max}}{p_{\max}^{\max}} \quad (116)$$

$$\Phi_s = \frac{6880}{2} \frac{4.98 - .731 - .212}{4.98} \quad (117)$$

$$\Phi_s = \frac{6880}{2} \frac{4.04}{4.98} = 2790 \text{ Maxwells}$$

and

$$B = \frac{\Phi}{A} = \frac{2790}{(.36)(.07)(2.54)(2.54)} = 17,200 \text{ gauss} \quad (118)$$

Since permalloy saturates at 16,000 gauss, the keeper cross section need be increased by only 7% to take full advantage of the available flux at the given reed displacement. This change alone, of course, would do no good unless the reed thickness were doubled as well, as we have already shown.

#### EXPERIMENTAL CHECK OF CALCULATIONS

To test the validity of the foregoing calculations, a series of measurements was made to determine the maximum voltage output as a function of reed displacement under conditions for which there is no magnetic saturation. The reed displacement was measured by "stopping" the vibrating reed at its maximum displacement (a) with a strobe light and then measuring (a) with a telemicroscope equipped with a calibrated micrometer screw.

The results of this experiment are shown in Fig. 10 where they are compared with the theoretical curve plotted from results of the computer calculations listed in Appendix II. As is apparent from Fig. 10, agreement is excellent considering the many approximations used in the calculations and that (a) can be measured with a precision of no better than ten to fifteen percent.

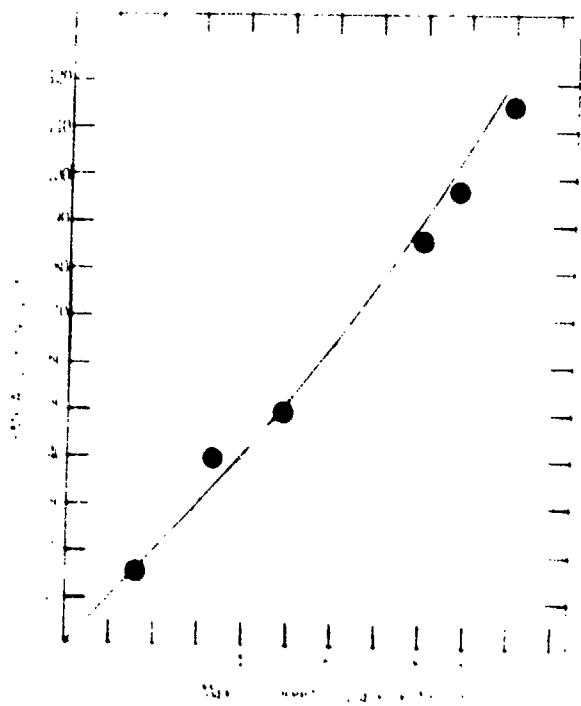


Fig. 10. Comparison of Experimental Points (dots) with Theoretical EMF-Displacement Curve (solid curve)

#### LOSSES IN THE REED

It is of interest to know how much electrical energy is dissipated in the reed through eddy current losses and hysteresis. The expression for the eddy current power dissipation in watts (see Appendix I) is

$$\frac{P_E}{n} = \frac{\pi^2 f^2 B_m^2 \cdot^3 l w}{6 \times 10^{16}} = \frac{\cdot^2 f^2 B_m^2 \cdot^2 V}{6 \times 10^{16}} \quad (119)$$

where  $n$  is number of laminations,  $f$  is the frequency,  $B_m$  is the flux density amplitude in gauss,  $\cdot$  is the lamination thickness,  $l$  and  $w$  are the reed length and width respectively,  $V$  is the lamination volume, and  $\cdot$  is the resistivity in ohm-cm. The reed dimensions are all measured in centimeters and the power is in watts. Since the reed is composed of two laminations each of the thickness  $\cdot = .0406$  cm, we multiply (119) by two and insert .0406 for  $\cdot$  as well as the appropriate values of the other parameters under saturation conditions.

$$P_E = .34 \text{ watts} \quad (120)$$

The expression for hysteresis power loss in the reed is given by

$$P_H = \pi f^2 \left( \frac{B_m}{8} \right)^{1.6} \quad \text{and} \quad P_H = \pi f^2 \left( \frac{B_m}{8} \right)^{1.6} V \quad (121)$$

where  $V = .0706 \text{ cc.}$   $V$  is a constant depending on the material and is .002 for our reed. Making the proper insertions gives us

$$P_H = (.002)(1500)(1500) \left( \frac{19.9}{10^5} \right)^{1.6} (.0706)$$

$$P_H = \frac{(.002)(1500)(1500)(1200)(.0706)}{10^{10}}$$

$$P_H = .00004 \text{ watts which is negligible.} \quad (122)$$

The eddy current losses, however, could become quite significant if the reed were not properly laminated. For example, an unlaminated reed of the same thickness as the laminated one would have four times the eddy current loss. It is, therefore, important that if the reed thickness is increased as recommended, it be done by adding laminations. A solid unlaminated reed of twice the thickness of the one presently used would have a power loss of about 1 watts, whereas a fourfold lamination of such a reed would reduce the loss to about .68 watts.

#### LOSSES IN THE KEEPER

Eddy current losses in the keeper come about because of fluctuations in the flux density as the magnet load line changes with the vibration of the reed. If the keeper thickness is increased by the required 7%, or better still, widened at the narrow points which saturate by 7%, the maximum flux density would be no more than 16,000 gauss. The operating conditions would then be optimized and it would be useful to have some estimate as to the eddy current losses. Such an estimate would be very rough since it is very difficult to determine the flux pattern in the keeper. We already know that when the reed is at its greatest displacement the flux carried by the narrowest portions of the keeper would be 16,000 gauss. We also need the flux density when the reed is in its equilibrium position. This is obtained by substituting the appropriate equilibrium values of the parameters in Eqs. (116 - 118). In this fashion we obtain

$$\Phi_K^E = \frac{\Phi_t^E}{2} \frac{P_t^E - P_{m4} - P_{y4}}{P_t^E}$$

$$\Phi_K^E = \frac{(2950)(2.17)}{2} \frac{4.23 - .731 - .212}{4.23} = 2490 \text{ Maxwells} \quad (123)$$

The cross-section dimensions of the keeper are .914 cm and .178 cm, so

$$B_K^E = \frac{2490}{(.914)(.178)} = 15,300 \text{ gauss}$$

Therefore, the field at the narrowest portion of the keeper fluctuates from 15,300 gauss to 16,000 gauss with an amplitude of  $\frac{700}{2} = 350$  gauss. The fluctuation in other parts of the keeper would be somewhat smaller, but 350 gauss can be used to get an upper limit for the expected losses. To this end we use Eq. (119) with the appropriate constants for the keeper whose volume is 2.44 cc and whose thickness would be .178 cm. Further, the fluctuation frequency of  $B_K^E$  is double that of the reed since  $B_K^E$  is a maximum at both ends of the reed's vibrational cycle. Using these values in Eq. (119) yields:

$$P_E = \frac{(3.14)(3.14)(3000)(3000)(350)(350)(.178)(.178)(2.44)}{(6)(45)10^{16}} 10^6$$

$$P_E = .31 \text{ watts} \quad (124)$$

which is about 2% of the expected optimum output. This loss of electrical energy can be avoided by a double lamination of the keeper to cut the loss to 0.08 watts or even a quadruple lamination which would result in the low eddy current loss of 0.02 watts. Since these numbers represent only upper limits, the actual values would probably be much smaller. The use of high-resistivity, high-permeability composite castings for the keepers would probably eliminate the eddy current losses entirely.

The hysteresis loss in the keeper cannot be obtained directly from Eq. (121) because the field in the keeper varies only over positive values of  $B$ , while (121) applies only to complete cycles about the principal hysteresis loops. We can, however, get some idea as to the order of magnitude of the loss by substituting our amplitude 350 gauss into (121). Using the value  $\mu = .0001$  for permalloy we have

$$P_H = (.0001)(3000)(3000) \left( \frac{350}{10^8} \right)^{1.6} (2.44) \quad (125)$$

$$P_H = 4.1 \times 10^{-6} \text{ watts} \quad (126)$$

which as in the case of the reed is negligible.

#### SUMMARY AND RECOMMENDATIONS

(1) Under the present conditions of operation the fluidic generator is producing only about 35% of its potential power output. Doubling the cross-section of the reed by adding lamination or increasing its width would augment its flux carrying capability to where the potential power output could be fully realized with only negligible eddy current and hysteresis losses in the reed. Appropriate adjustments in gap length would also be necessary to prevent saturation and to allow sufficient latitude for vibration.

(2) Keeper hysteresis losses are also negligible but eddy current losses can be appreciable unless the keeper is laminated or made of a suitable composite material. Further, the narrowest part of the keeper cross section must be increased by about 7%, to avoid saturation with the given reed displacement amplitude of .017'.

(3) To facilitate design optimization of future generators a computer study was done to obtain a series of design matrices which list voltage amplitude as a function of gap length ( $l_g$ ), reed thickness ( $\tau$ ), and reed displacement amplitude (a). The computer program uses the mathematical procedure of the sample calculation made in this report and it is written in Fortran IV for the Burroughs 5500 Computer. The program is reproduced in Appendix II together with a summary of the equations used in the calculations.

The computed voltage amplitudes are listed in Table II in Appendix II. All of the listed voltages are calculated for a 1500 turn coil, a reed width of .27', a reed vibrational frequency of 1500 hertz, and the standard magnet and keeper dimensions used in the sample calculation and summarized in Table I. The assumption is also made that the keeper does not saturate for any of the parameter choices listed. This assumption, as we have shown in the sample, is not valid for the larger values of (a) unless the keeper thickness is increased by an appropriate amount. This thickening of the keeper would, of course, affect the value of  $P_{y4}$  and hence the permeance calculations. The effect on the calculated voltage output, however, is not likely to be significant because in the sample calculation  $P_{y4}$  is only of the order of 10% of  $P_4$ , and  $P_4$  in turn constitutes only about 40% of  $P_t$ . Furthermore,  $P_{y4}$  itself is relatively insensitive to keeper thickness ( $W$ ) since  $W$  appears only in a small correction to the logarithmic factor in Eq. (13). Hence, thickening of the keeper to required values will probably not affect the calculated voltages by more than the order of a percent or two even in the worst cases.

The calculations also assume infinite reed permeability and the values not actually attainable with the reed material used are marked with an asterisk. Thus the design can easily be optimized by choosing the parameters yielding the largest non-asterisked voltage in the Tables. This, of course, is always subject to the condition that the reed of requisite thickness can be driven with the stated amplitude and frequency. Perhaps this can be assured in many cases by making appropriate adjustments of the reed stiffness through variation of the reed material and dimensions at the point where it is anchored or by widening the reed rather than thickening it.

The Tables can be used to obtain the power output in any load resistance  $R_L$  from Eq. (126), viz.

$$P_L = \frac{V_{max}^2 R_L}{2Z^2} \quad (127)$$

where  $Z$  is the total circuit impedance obtained from Eqs. (109) and (110). The coil inductance is a function of reed thickness and the empirical curve of the relationship is shown in Fig. 11. As is evident from (111), however, the reactive portion of the impedance is only about a percent and a half of the total, and the variation of reactance with reed thickness will not have a significant effect upon power output at the frequency and resistance used.

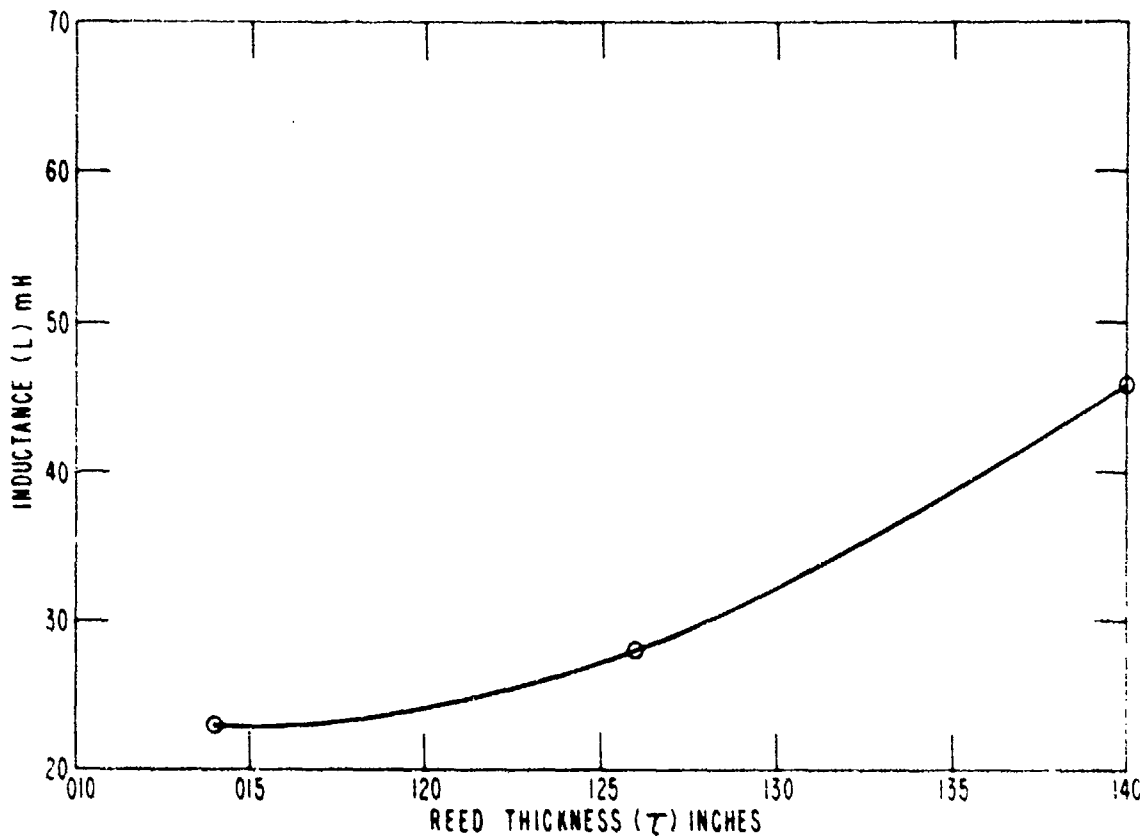


Fig. 11. Inductance of Sensing Coil as a Function of Reed Thickness.

(4) The present configuration of the magnetic circuit results in relatively low-sloped load lines which intersect the Alnico 5 demagnetization curve well below its "knee" (Fig. 9). Note that if Co<sub>5</sub>Sm were used in place of Alnico 5 much higher flux densities would result for any given load line with a concomitant increase in power output. This, of course, is always assuming that neither reed nor keeper are saturated. It probably would be most practical to keep the power output at about 10-12 watts with the use of much less magnetic material through substitution of Co<sub>5</sub>Sm. A more compact generator operating at lower load lines with the same power output could probably be designed using the latter material.

(5) A composite material consisting of permalloy particles densely packed in a nonconducting binder might be desirable for the keeper. Providing a sufficiently high packing density is obtainable, eddy current losses could be virtually eliminated without too great a loss in flux-carrying capability. Such a composite could also be press molded into the desired shape thus improving the efficiency of fabrication.

## APPENDIX I

### DERIVATION OF THE FORMULA FOR ENERGY LOSS THROUGH EDDY CURRENTS

Consider a sheet of metal such as the one pictured in Fig. 12. The length  $l$  is much larger than the thickness  $t$  and the width  $w$  is arbitrary. A sinusoidal field  $B$  is acting in the  $y$  direction as shown. The varying field  $B$  will induce EMFs which will give rise to circulating or eddy currents. We wish to find the power expended by these currents. We proceed by considering a current loop indicated by the arrows in Fig. 12. The EMF around this loop is then given by

$$V = \frac{d\Phi}{dt} = \frac{AdB}{dt} = \frac{2lx}{8} \frac{dB}{dt} \quad (128)$$

If we neglect the small voltage drops across the width of the loop at the ends we can write for the voltage drop per unit length in the  $z$  direction

$$v = \frac{V}{2l} = \frac{xB}{8} \frac{dB}{dt} \quad (129)$$

The current density  $i$  is then obtained from the relation

$$i = \frac{v}{\rho} \quad (130)$$

where  $\rho$  is the resistivity of the material. Substituting (129) in (130) yields

$$i = \frac{x}{10\rho} \frac{dB}{dt} = \frac{xB_{\max}}{8 \cdot 10^8} \cos \omega t \quad (131)$$

The instantaneous power,  $dP$ , dissipated in the unit laminar element  $dx$  is then

$$dP = w \rho i^2 dx = \frac{w x^2 B_{\max}^2}{8 \cdot 10^{16}} \cos^2 \omega t$$

$$dP = \frac{w t^2 B_{\max}^2}{16} x^2 dx \cos^2 \omega t \quad (132)$$

and the total power loss,  $P$ , of a unit length of sheet is

$$P = \int_{-\frac{t}{2}}^{\frac{t}{2}} dP = \frac{w t^2 B_{\max}^2}{32 \cdot 10^{16}} \left| x^3 \right|_{-\frac{t}{2}}^{\frac{t}{2}} \cos^2 \omega t \quad (133)$$

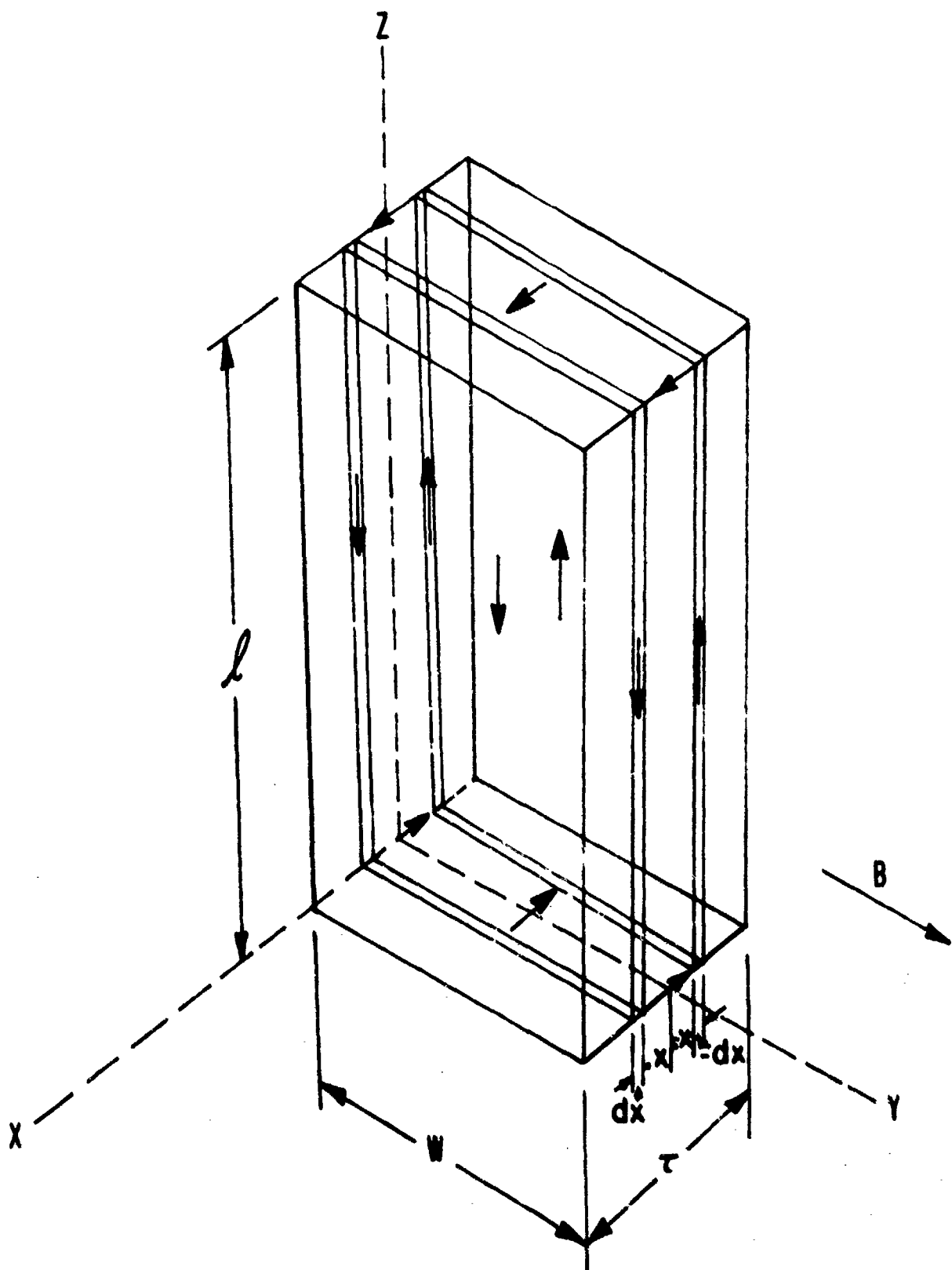


Fig. 12. Derivation of the Eddy Current Loss Formula.

$$P = \frac{\omega^2 B_{\max}^2 \tau^3}{3 \cdot 10^{16} \cdot 4} \cos^2 \omega t = \frac{\omega^2 B_{\max}^2 \tau^3}{12 \cdot 10^{16}} \cos^2 \omega t \quad (134)$$

The energy loss per cycle is then given by

$$w_c = \frac{\omega^2 B_{\max}^2 \tau^3}{12 \cdot 10^{16}} \int_0^{\frac{2\pi}{\omega}} \cos^2(\omega t) (\omega dt) \quad (135)$$

$$w_c = \frac{\pi \omega \tau^3 B_{\max}^2}{12 \cdot 10^{16}} \quad (136)$$

The average power per unit length of sheet is

$$\bar{P} = f w_c = \frac{f \pi \tau^3 B_{\max}^2}{12 \cdot 10^{16}} = \frac{\pi^2 f^2 \tau^3 B_{\max}^2}{6 \cdot 10^{16}} \quad (137)$$

The average power for the entire length of the sheet is then

$$\bar{P}_t = f \bar{P} = \frac{\pi^2 f^2 \tau^2 B_{\max}^2 \ell \omega \tau}{6 \cdot 10^{16}} = \frac{\pi^2 f^2 \tau^2 B_{\max}^2 V}{6 \cdot 10^{16}} \quad (138)$$

where  $V$  is the volume of the sheet.

## APPENDIX II

### SUMMARY OF COMPUTATIONAL PROCEDURE IN CALCULATION OF PEAK VOLTAGE AND ADAPTATION TO COMPUTER PROGRAM

All relevant permeances are calculated for the generator with the reed in the equilibrium position. There are five such permeances of which four are associated with the four air gaps and the fifth with the magnetic leakage paths. The two gaps at the fixed end of the reed are always equal and the associated permeances are equal and denoted by  $P_3$ .  $P_1$  and  $P_2$  refer to the gaps at the vibrating end of the reed.  $P_4$  is the permeance of the composite of all leakage paths.  $P_3$  has five components and we can write for the equilibrium condition:

$$P_3 = P_{G3} + P_{E3} + P_{F3} + P_{L3} + P_{W3}$$

all of which are illustrated in Fig. 5 and are computed by the following formulae as functions of  $f_g$ ,  $t$  and  $a$ . All other dimensions are fixed and are the same as those of the sample calculations.

$$P_{G3} = \frac{.0408}{f_g - t}$$

$$P_{E3} = .0364$$

$$P_{F3} = .303$$

$$P_{L3} = .215 \ln \left( 1 + \frac{.30}{f_g - t} \right) + [.213 - .0916(f_g - t)] \ln \left( \frac{.30}{f_g - t} \right)$$

$$P_{W3} = .0445 \ln \left( 1 + \frac{1.73 t}{f_g - t} \right)$$

$P_4$  has five components and is given by

$$P_4 = P_{P4} + P_{y4} + P_{M4} + P_{L4} + P_{W4}$$

and

$$P_{P4} = .647"$$

$$P_{y4} = .212"$$

$$P_{M4} = .731"$$

$$P_{L4} = .136$$

$$P_{W4} = .134 \ln \frac{.4 + 1.16 f_g}{t + 1.16 f_g}$$

$P_1$  and  $P_2$  have the same form with either always reaching its maximum when the other is at its minimum. Each has 5 components and

$$P_1 = P_{G1} + P_{E1} + P_{F1} + P_{L1} + P_{W1}$$

$$P_{G1}^{\max} = P_{G2}^{\min} = \frac{.0408}{l_g - t \mp 2a}$$

$$P_{E1} = P_{E2} = .0364"$$

$$P_{F1} = P_{F2} = .303"$$

$$P_{L1}^{\max} = P_{L2}^{\min} = .215 \ln \left( 1 + \frac{.30}{l_g - t \mp 2a} \right)$$

$$+ [ .170 - .0918(l_g - t \mp 2a) ] \frac{.30}{l_g - t \mp 2a}$$

$$P_{W1}^{\max} = P_{W2}^{\min} = .0445 \ln \left( 1 + \frac{1.73 t}{l_g - t \mp 2a} \right)$$

The total permeance of the magnetic circuit  $P_t$  is then given by the formula:

$$P_t = P_4 + \frac{(P_1 + P_3)(P_2 + P_3)}{P_1 + P_2 + 2P_3}$$

and both the equilibrium and full reed displacement values of  $P_t$  are calculated. We use the equilibrium value  $P_E$  to obtain our load line slope  $B/H$  via the formula

$$\left( \frac{B}{H} \right)^E = - \frac{l}{A} P_E$$

where  $l$  and  $A$  are respectively the length and cross-sectional area of the magnet.

The intersection of this load line with the demagnetization curve of Alnico 5 is the base point of the recoil line (slope 4.3 for Alnico 5) along which the system then operates. The recoil line is thus of the form:

$$B = 4.3 H + B_0$$

where  $B_0$  is determined from the base point. The maximum value of  $P_t$  corresponding to full displacement is then used in the relation

$$\left( \frac{B}{H} \right)^{\max} = - \frac{l}{A} P_t^{\max}$$

to obtain the new load line. The intersection of this load line with the recoil line already determined yields the maximum value of  $B$  in the magnet.

The corresponding total available flux is then given by

$$\Phi_t^{\max} = B^{\max} A_{\text{magnet}}$$

and the flux amplitude in the reed can then be calculated from the relation

$$\Phi_R^{\max} = \Phi_t^{\max} \frac{P_3(P_1 - P_2)}{(P_1 + P_3)(P_2 + P_3) + P_4(P_1 + 2P_3 + P_2)}$$

The induced voltage amplitude is then obtained from

$$V^{\max} = \frac{N_w \Phi_R^{\max}}{8}$$

The computer program which follows this procedure is reproduced below in Fortran IV. In addition to calculating the expected voltage for a given set of parameters, the program also instructs the computer to calculate

$$B_R^{\max} = \frac{\Phi_R^{\max}}{10}$$

If the result is larger than the saturation flux density of the reed material (19,900 gauss), the calculated voltage is not attainable and is marked with an asterisk in Table I.

COMPUTER PROGRAM USED TO OBTAIN TABLE II

```

FILE 1*FILE)OUNTTPRINTER
      REAL MAX,PM4,PM4,PF4,PF4A,PL4,PA,PG3,PF3,PF3,PI3,PN3,P3,PTF,
      X,M,PL,LG
      DIMENSION H(6),R(6),P(3),F(3),VOLT(3E),BPFEN(35),ASTK(24)
      DATA (BFT),T=1,A)/1000,0000,0000,10000,11000,12000/
      (HFT),T=1,A)/617.0,563.0,546.0,820.0,817.0,200.0/
      Z=1210,
      RI=600,
      THNS=1500,
      OMGR=30000+3,1415926
      FF 10 L0,000,0010,005
      WRITE(1,800) 10
500 FORMAT(1X,1X(1X,/)1X,"GENERATOR OUTPUT IN VOLTS AC FOR GAP ="
      LENGTH = #5.3+2X,"TCHFS",//)
      WRITE(1,807)
      97 FORMAT(2Y,"PFEDR",2Y,/,1Y,"THTPKNS",1Y,
      "AMPITUDE IN TCHFS",/,1X,PCTNCHFS10,1X,".001.000,003.004"
      ".005.008.007.008.009.010.011.012.013.014.015.016.017.018.019"
      ".020.021.022.023.024.025.026.027.028.029",//)
      FF 110 T=.01,1E-,005+0.002
      N=6
      X=EL0+T/2,-.001
      IF(XK,GT,0,020) X=.00.020
      FF 120 T=.001,YN,0.001
      N=N+1
      ACTR(M)=0
      PM4=.133*ALN((.8+1.154i6)/(7+1.154i6))
      PM4=.731
      PP4=.445
      PY4=.212
      PI4=.134
      P05P,P+PM4+PP4+PY4+PL4
      Z=L0**7
      PG3=.00077
      PF3=.034
      FF3=.0029
      PPF=.215*ALOG(1.+3r/2)
      C=(.2128-.0916*Z)*ALOG(.30/2)
      PI3=PP+G
      FF3=.044*2+ALOG(1.+((1.772+T)/2))
      P3=PG3+PF3+PL3+PM3
      F(1)=1.G**2+.A
      F(2)=1.G**2+.A
      F(3)=1.G**3
      FF 35 1E+3
      G=.33034,.04452*ALN((1.+((1.732+T)/2)/F(1))+(.04078/F(1))
      P=.215*ALN((1.+((3/F(1)))
      F(1)=F(1)+.1899+.0616*F(1))+.01PGC(.3/F(1))
35  CONTINUE
      PTE=PF4+PF4+PF3)/2.
      PPF= -1.172*PTF
      K=ARS(304E)
      IF((X<1.7,18,18) GE 10) T= 5
      IF((X<1.8,18,18) AND. K<LT.16,18) GO TO 10
      IF((X<1.8,18,19) AND. K<LT.19,23) GO TO 19
      IF((X<1.8,19,22) AND. K<LT.26,38) GO TO 20
      IF((X<1.8,26,38) AND. K<LT.40,1) GO TO 28
      T=7
      GO TO 50
      5 1=2
      GO TO 50
      10 1=3
      39
      00000100
      00000200
      00000300
      00000400
      00000500
      00000600
      00000700
      00000800
      00000900
      00001000
      00001100
      00001200
      00001300
      00001400
      00001500
      00001600
      00001700
      00001800
      00001900
      00002000
      00002100
      00002200
      00002300
      00002400
      00002500
      00002600
      00002700
      00002800
      00002900
      00003000
      00003100
      00003200
      00003300
      00003400
      00003500
      00003600
      00003700
      00003800
      00003900
      00004000
      00004100
      00004200
      00004300
      00004400
      00004500
      00004600
      00004700
      00004800
      00004900
      00005000
      00005100
      00005200
      00005300
      00005400
      00005500
      00005600
      00005700
      00005800
      00005900
      00006000
      00006100
      00006200

```

50 TC 50	00006300
15 T*4	00006400
50 TC 50	00006500
20 T*5	00006600
50 TC 50	00006700
25 T*4	00006800
50 H(E(I))-P(I-1))/ (E(I)-H(I-1))	00006900
HME=(P(I)-H(I))/ (I,-H/BHFE)	00007000
PHSF=4,3*(HME/BHFE)	00007100
• P(1)*P1, P(2)*P2, P(3)*P3 WHEN A=0	00007200
P=(P(1)+P2)+(P2+P3)	00007300
E=(P1+P2)+2.*P3	00007400
PHMAX=1,172*(P4+P5/E)	00007500
PHAY=80/(1,-4,3*PHMAX)	00007600
FLUYTH=2,17*PHAY	00007700
FLUYTH=FLUYTH*(P(1)-P(2))/(P+P4+P5)	00007800
MAX=10000,	00007900
IF(PHAY>10),GT,MAX) ACTH(N)=PHAY	00008000
IF(PHAY>10),GT,MAX)	00008100
120 DATA	00008200
WRITE(F1+13),FLUYTH,ACTH(N),T01+1	00008300
13 F01=AT(AY,F0,2,3Y,31(I3+A1))	00008400
300 F0=AT(F11,2)	00008500
110 DATA	00008600
100 DATA	00008700
STOP	00008800
END	00008900

TABLE II

Voltage outputs for various gap lengths, reed thicknesses and reed displacement amplitudes.  
 The values marked with an asterisk are not attainable with the reed material presently in use.  
 They are the values to be expected with the use of reed material that does not saturate under  
 the given operating conditions.

GAP LENGTH, INPUT VOLTAGE AT 1000 CPS = 0.0001 INCHES

REED THICKNESS (INCHES)	AMPLITUDE, IN INCHES	VOLTAGE										
*0.010	0.1	26	5.1	6.7	0.10	1.0	0.10	1.0	0.10	1.0	0.10	1.0
*0.012	0.2	20	6.6	7.0	0.20	1.2	0.20	1.2	0.20	1.2	0.20	1.2
*0.014	0.4	13	5.1	6.7	0.40	1.1	0.40	1.1	0.40	1.1	0.40	1.1
*0.016	0.9	3.8	5.0	5.2	0.90	1.1	0.90	1.1	0.90	1.1	0.90	1.1
*0.018	1.2	4.5	6.9	7.0	1.20	1.2	1.20	1.2	1.20	1.2	1.20	1.2
*0.020	0.7	5.4	7.3	7.5	0.70	1.5	0.70	1.5	0.70	1.5	0.70	1.5
*0.022	0.2	6.6	10.2	14.1	0.20	1.6	0.20	1.6	0.20	1.6	0.20	1.6
*0.024	1.0	1.7	12.0	12.0	1.00	3.2	1.00	3.2	1.00	3.2	1.00	3.2
*0.026	1.1	1.6	16.0	24.1	1.10	4.0	1.10	4.0	1.10	4.0	1.10	4.0
*0.028	1.0	1.8	23.2	31.7	0.50	5.0	0.50	5.0	0.50	5.0	0.50	5.0
*0.030	1.0	2.6	34.5	52.0	0.50	8.0	0.50	8.0	0.50	8.0	0.50	8.0
*0.032	1.0	3.0	32.0	50.0	0.50	10.0	0.50	10.0	0.50	10.0	0.50	10.0
*0.034	1.0	3.4	24.0	46.0	0.50	12.0	0.50	12.0	0.50	12.0	0.50	12.0

TABLE II (cont'd)

CONTINUATION OF TABLE II (CONT'D) FOR RAPID RATES OF REACTION

REF.	10 <sup>3</sup> ( $\Delta E_{rx}$ ) Kcal/mole	10 <sup>3</sup> ( $\Delta S_{rx}$ ) E.U.	10 <sup>3</sup> ( $\Delta H_{rx}$ ) Kcal/mole	10 <sup>3</sup> ( $\Delta F_{rx}$ ) Kcal/mole	10 <sup>3</sup> ( $\Delta G_{rx}$ ) Kcal/mole	10 <sup>3</sup> ( $\Delta H_{rx}$ ) Kcal/mole	10 <sup>3</sup> ( $\Delta G_{rx}$ ) Kcal/mole	10 <sup>3</sup> ( $\Delta F_{rx}$ ) Kcal/mole	10 <sup>3</sup> ( $\Delta G_{rx}$ ) Kcal/mole
•C11	11	19	64	600	740	670	740	600	740
•C12	11	22	64	54	84	40	84	54	84
•C14	12	26	57	54	63	78	66	51	78
•C16	14	27	61	64	72	60	72	60	72
•P11	15	31	67	62	62	52	62	52	62
•P21	15	31	67	62	62	52	62	52	62
•P62	17	49	64	PA	PA	PA	PA	PA	PA
•P23	20	60	76	165	117	175	221	178	221
•P24	20	60	92	124	161	272	225	377	225
•P25	26	74	114	16	16	214	288	340	288
•P31	25	91	146	21	21	220	241	21	220
•P32	40	123	196	24	24	197	24	197	24
•P34	81	170	279	430	PA	PA	PA	PA	PA
•P36	119	256	446	PA	PA	PA	PA	PA	PA
•P38	163	435	PA						
•P40	375	PA	PA	PA	PA	PA	PA	PA	PA

TABLE II (cont'd)

תְּנַתֵּן לְעֵמֶקֶת אֶת-מִזְרָחֶךָ וְלַמְּלֵאָה אֶת-מִזְרָחֶךָ

TABLE II (cont'd)

THE PRACTICAL: 1911-12  
THE PRACTICAL: 1912-13

TABLE II (cont'd)

卷之三

TABLE II (cont'd)

SUSCEPTIBILITY OF C. ALBICANS TO 10<sup>-4</sup> MOL/L CTRW = 0.0005, THERM.

THERMOTOLERANCE	SUSCEPTIBILITY TO 10 <sup>-4</sup> MOL/L CTRW									
	0.01	0.02	0.03	0.04	0.05	0.06	0.07	0.08	0.09	0.10
0.010	0	13	14	15	16	17	17	17	17	17
0.012	0	14	15	16	17	18	18	18	18	18
0.014	0	15	16	17	18	19	19	19	19	19
0.016	0	16	17	18	19	20	20	20	20	20
0.018	0	17	18	19	20	21	21	21	21	21
0.020	0	18	19	20	21	22	22	22	22	22
0.022	0	19	20	21	22	23	23	23	23	23
0.024	0	20	21	22	23	24	24	24	24	24
0.026	0	21	22	23	24	25	25	25	25	25
0.028	0	22	23	24	25	26	26	26	26	26
0.030	0	23	24	25	26	27	27	27	27	27
0.032	0	24	25	26	27	28	28	28	28	28
0.034	0	25	26	27	28	29	29	29	29	29
0.036	0	26	27	28	29	30	30	30	30	30
0.038	0	27	28	29	30	31	31	31	31	31
0.040	0	28	29	30	31	32	32	32	32	32
0.042	0	29	30	31	32	33	33	33	33	33
0.044	0	30	31	32	33	34	34	34	34	34
0.046	0	31	32	33	34	35	35	35	35	35
0.048	0	32	33	34	35	36	36	36	36	36
0.050	0	33	34	35	36	37	37	37	37	37
0.052	0	34	35	36	37	38	38	38	38	38
0.054	0	35	36	37	38	39	39	39	39	39
0.056	0	36	37	38	39	40	40	40	40	40
0.058	0	37	38	39	40	41	41	41	41	41
0.060	0	38	39	40	41	42	42	42	42	42

TABLE II (cont'd)

CONFIDENTIAL 2010 RELEASE UNDER E.O. 14176

TABLE II (cont'd)

GENERATOR OUTPUT IN VOLTS: AIR FLOW 600 L/SEC = 0.075 TURBINE

REF ID	WICHITA	CHICAGO	AMPLITUDE, 1000 CYCLES	1000 CYCLES	100 CYCLES	10 CYCLES	1 CYCLE
013	7	10	13	14	20	25	27
014	6	7	11	15	27	35	37
015	4	4	8	12	26	37	42
016	4	4	8	12	26	35	40
017	4	4	8	13	21	30	35
018	4	4	8	13	21	30	35
019	4	4	8	13	21	30	35
020	4	4	8	13	21	32	37
021	4	4	8	14	21	32	37
022	4	5	10	15	20	32	39
023	5	10	15	21	31	42	43
024	5	10	15	21	31	42	45
025	5	11	16	22	34	40	46
026	5	11	16	22	34	40	46
027	5	12	18	24	34	42	47
028	5	12	18	24	34	42	47
029	5	13	19	24	32	40	46
030	5	13	19	24	32	40	46
031	5	14	21	28	35	42	49
032	7	14	21	28	35	42	50
033	7	14	22	30	38	46	52
034	8	14	22	30	38	46	52
035	8	14	24	33	42	51	57
036	8	14	24	33	42	51	57
037	9	15	24	34	44	54	62
038	9	15	24	34	44	54	62
039	10	20	30	40	50	60	67
040	10	20	30	40	50	60	67
041	11	22	33	45	57	70	81
042	12	24	37	50	64	76	87
043	12	24	37	50	64	76	87
044	14	27	42	57	72	90	105
045	14	27	42	57	72	90	105
046	15	31	46	65	83	103	120
047	15	31	46	65	83	103	120
048	16	34	55	75	97	121	140
049	16	34	55	75	97	121	140
050	21	42	64	88	114	144	170
051	21	42	64	88	114	144	170
052	22	49	76	105	137	174	222
053	22	49	76	105	137	174	222
054	22	50	92	124	170	221	266
055	22	50	92	124	170	221	266
056	23	53	141	161	197	237	286
057	23	53	141	161	197	237	286
058	24	56	145	166	198	239	289
059	24	56	145	166	198	239	289
060	26	60	145	166	198	239	289
061	26	60	145	166	198	239	289
062	27	62	149	170	202	244	296
063	27	62	149	170	202	244	296
064	27	62	149	170	202	244	296
065	27	62	149	170	202	244	296
066	27	62	149	170	202	244	296
067	27	62	149	170	202	244	296

TABLE II (cont'd)

CONFIDENTIAL - DRAFT - 1974 - FOR RAP EFFECT - 0.000 INCHES